2022-08-28

A Review on the Modelling of Wave-Structure Interactions Based on OpenFOAM

Huang, L

10.51560/ofj.v2.65
OpenFOAM Journal
OpenCFD Ltd

A review on the modelling of wave-structure interactions based on OpenFOAM

Abstract: The modelling of wave-structure interaction (WSI) has significant applications in understanding natural processes as well as securing the safety and efficiency of marine engineering. Based on the technique of Computational Fluid Dynamics (CFD) and the open-source simulation framework - OpenFOAM, this paper provides a state-of-the-art review of WSI modelling methods. The review categorises WSI scenarios and suggests their suitable computational approaches, concerning a rigid, deformable or porous structure in regular, irregular, non-breaking or breaking waves. Extensions of WSI modelling for wave-structure-seabed interactions and various wave energy converters are also introduced. As a result, the present review aims to help understand the CFD modelling of WSI and guide the use of OpenFOAM for target WSI problems.

Keywords: Wave-structure interaction; Computational Fluid Dynamics; OpenFOAM.

1. Introduction

1.1 Background

Wave-Structure Interaction (WSI) is defined as ocean waves applying forces to one or multiple solid bodies and the solid's dynamic response changes the surrounding wave field simultaneously. WSI processes are ubiquitous in both marine environment and engineering, e.g. influencing the distribution of sea ice and vegetation, and dictating the safety and performance of ships and offshore installations. Thereby, the modelling of WSI is of great importance for marine science, design and operations.

WSI modelling has been categorised into one-way coupling and two-way coupling. In one-way coupling, the fluid impacts the structure, but not the other way around. In two-way coupling models, the fluid and the structure impact each other. The modelling started with analytical approaches. Initially, mathematical equations were developed to describe ocean waves as a periodic movement along a timeline. Those wave equations were used to calculate the harmonic wave loads on a structure, or wave-induced structural motions. Subsequently, the wave diffraction by a structure was also formulated. Such analytical solutions for WSI have been developed since the early 20th century and approached a degree of maturity around the 1990s, with a wide range of problems addressed by the Morison equation and the potential flow theory coupled with structural solutions [1–5]. However, most analytical WSI works were limited to linear wave conditions and inviscid fluids to obtain closed-form solutions, only valid for small-amplitude waves.

Since the 2000s, nonlinear wave modelling has become popular using the potential flow theory in combination with higher-order Boundary Element Methods (BEM). This BEM approach allows the prediction of high-steepness waves and the corresponding response of structures, which has shown good accuracy against experiments so long as the wave does not break by itself or by the structure [6,7]. However, the BEM approach is based upon dimensionality reduction as the discretisation is applied on a boundary rather than on a volume. This limits the applicable structures to simple geometries, such as a cuboid, a cylinder or a sphere. Overall, the BEM approach still cannot model WSI phenomena that involve strong nonlinearities.

With the advances in modern computational techniques, computational fluid dynamics (CFD) models have been developed to address more realistic WSI problems. In CFD, the physical domain is represented by a corresponding computational domain, in which a solid geometry can be inserted. The space between the surface of the structure and the domain boundaries is the fluid field, which can be discretised and use the Navier-Stokes equations to obtain highly-nonlinear wave profiles.

There are two main branches of CFD, mesh-free methods and mesh-based methods. The computational speed has been a significant challenge for mesh-free methods, such as the Smoothed Particle Hydrodynamics (SPH), which represents the fluid and structure as particles, e.g. [8]. In addition, in SPH it is hard to develop boundary conditions such as inlet/outlet and the method requires artificial inputs for viscous effects [9]. These are significant challenges for WSI modelling, in which inlet/outlet and fluid viscosity are essential. Thus the WSI applicability of mesh-free methods is limited.

In terms of mesh-based methods of CFD, for example the Finite Volume Method (FVM), the solid geometry is modelled as a closed surface that is in contact with numerous computational cells to represent its structural complexity. In addition, a specific boundary-layer mesh can be built around the geometry to account for fluids' boundary-layer effect. Local mesh refinements are mature with FVM. These features render mesh-based CFD a suitable approach to model and analysing WSI problems, with the level of fidelity sufficiently high that the simulation can closely reproduce what happens in real sea states (See Figure 1 for an example).

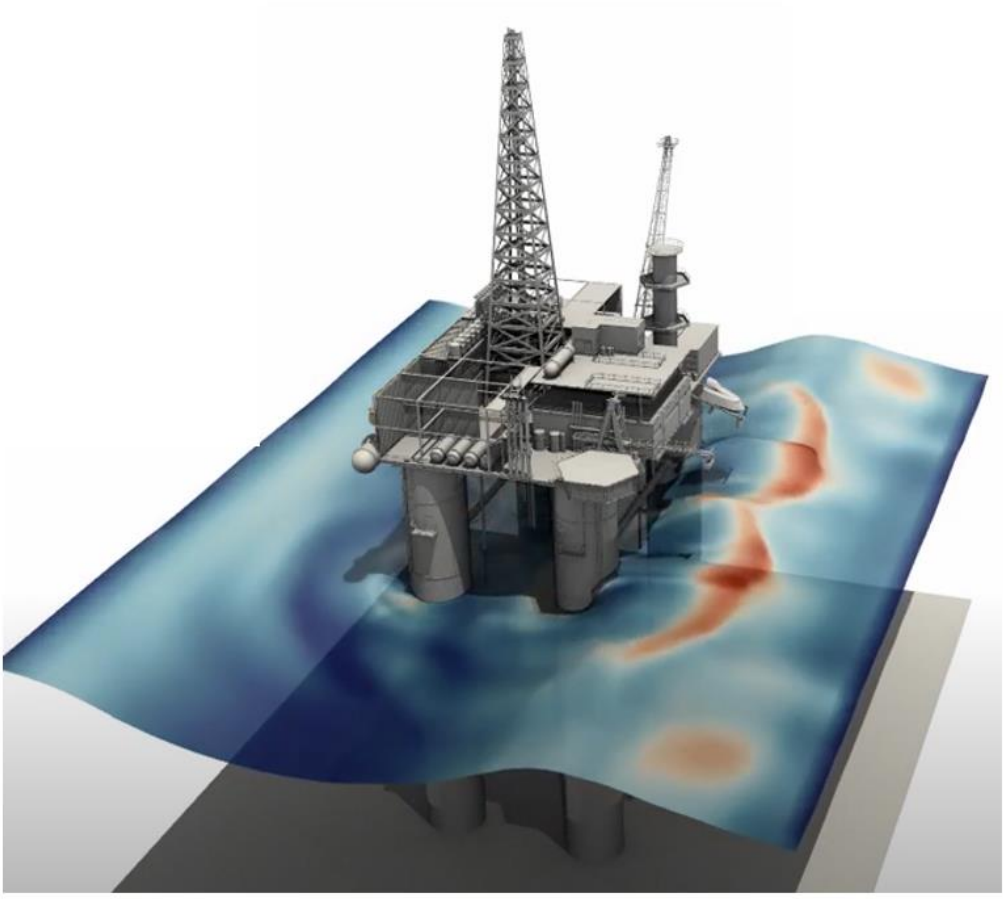

Figure 1: CFD simulation example of waves interacting with a realistic structure [10]

1.2 Choices of CFD software

Different software is available for WSI simulations, ranging from commercial and open-source software to in-house developments. Commercial tools commonly feature graphical user interfaces (GUIs) and often specific numerical methods, e.g. for multi-physics analysis. However, the often significant license fees and, to some extent, the restricted access to the source code, possibly hinders the usage of commercial software for WSI applications.

By avoiding license fees and providing access to source code, open-source CFD software has gained popularity and is commonly backed by active communities. For OpenFOAM, dedicated workshops and user group meetings facilitate knowledge exchange within the community, driving new developments. In addition, a few private companies, such as Engys or WIKKI, are heavily involved in code development. Drawbacks of using open-source software may arise from steep learning curves for beginners. Furthermore, developments of new (advanced) numerical tools lack profit as a motivator. However, unlimited access to the source code enables custom code development, facilitating the open-source software to be applied in a wide range of applications. Apart from OpenFOAM, there is also other open-source software that has made significant contributions to WSI modelling, such as REEF3D and Gerris [11,12].

In-house codes are either driven by specific (physical) problems or the desire to include advanced numerical algorithms. Their nature makes them unavailable to a large community. Examples of such codes can be found in [13,14].

The wide range of different CFD software suites raises the question of which one to select. Decision drivers of choosing a specific CFD software for WSI are diverse, ofter being the available turbulence models or numerical wave generation and absorption. Additional decision drivers may include project time frame, budget, and user experience.

In principle, there is not a function that is implemented in commercial software that cannot be implemented in OpenFOAM, and vice versa. The main differences, on one hand, include that OpenFOAM enables more possibilities for learning and research purposes, as it is completely free to view and develop the code. On the other hand, the learning curve for OpenFOAM is known to be longer than commercial software, making it more challenging for a beginner who may have limited time for a specific project.

Some studies can be found which perform comparative analyses of different CFD software. Based on the analysis of extreme wave loading, Westphalen et al. [15] consider STAR-CCM+, ANSYS CFX, the in-house Cartesian cut-cell solver AMAZON-SC 3D, and an SPH solver. Sjökvist et al. [16,17] present a comparison of OpenFOAM with ANSYS Fluent. Most recently, the CCP-WSI Blind Test Series 1-3 [17–19] aimed at delivering comprehensive code-to-code

and code-to-experiment comparisons of different modelling approaches and dedicated experimental validation data. By way of example, Figure 2 shows the CFD software used for WSI simulations of Wave Energy Converters (WECs) and their relative popularity in the literature.

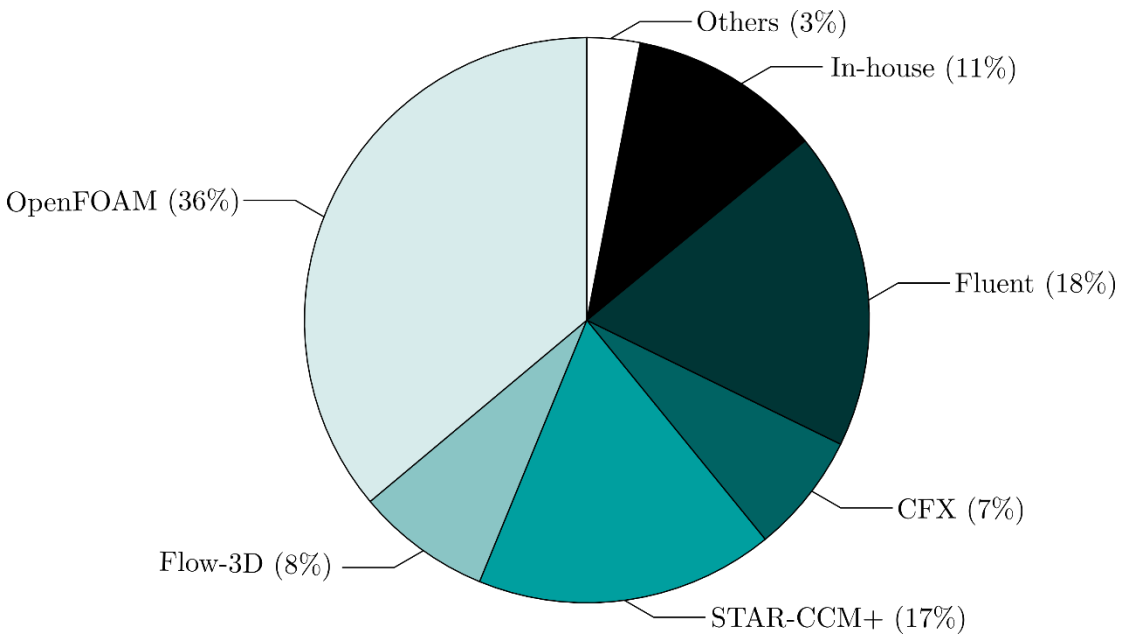

Figure 2: CFD software used for WSI simulations of WECs and their relative popularity among approximately 200 reviewed studies [21].

1.3 Scope of this paper

Although CFD simulations have been shown capable of modelling WSI, the quality of the simulations is dependent on the user's computational setups. The capabilities of CFD provide abundant options on numerical models and setups to account for the free surface, wave modelling, turbulence effect, and structural response, among others. When inappropriate setups are used, simulations can crash or lead to unphysical/erroneous results. For this reason, review articles can bring significant contributions by helping users understand CFD and providing recommendations on suitable modelling branches for specific problems.

In order to provide a comprehensive review of CFD modelling of WSI problems, the present work selects OpenFOAM as the framework. Based on the open-source code, primary WSI modelling approaches are reviewed and their applicability and limitation for various physical problems are discussed. This allows readers to refer to corresponding source code, gaining a deeper understanding than appreciating black-box functions in commercial CFD tools.

The remainder of this paper is organised as follows: Section 2 introduces relevant fluid modelling approaches, i.e. modelling different types of ocean surface waves. Section 3 reviews WSI modelling concerning various structural characteristics, for (3.1) rigid fixed structures, (3.2) rigid floating structures, (3.3) deformable structures, (3.4) porous structures; furthermore, (3.5) provides an extension of WSI modelling that couples with seabed response. Section 4 presents the modelling of various types of WECs, where the modelling methods of mooring lines and power-take-off systems are also introduced. Finally, Section 5 summarises this work with its main conclusions.

2. Wave flow

2.1 Free surface modelling

A key requirement for simulating water waves in OpenFOAM is modelling the evolving free surface interface. The most popular method for achieving this is the Volume of Fluid (VOF) approach, detailed in Section 2.1.1, which can simulate complex WSI problems such as those involving wave breaking, overtopping and slamming. Alternative methods are also available, as discussed in Section 2.1.2. These methods are not widely applicable as VOF but can be capable of modelling a restricted range of WSI conditions with potential computational savings.

2.1.1 The VOF method

The VOF method tracks the relative volumetric percentage of different fluids in each cell. For the case of wave simulations, the VOF method typically considers two fluid phases: water and air. This is depicted in Figure 3(a), where the volume fraction of water is displayed - a value of 1 corresponds to a cell containing 100% water, a value of 0 corresponds cells with 100% air, and a value between 0 and 1 represent the cells around the free surface interface.

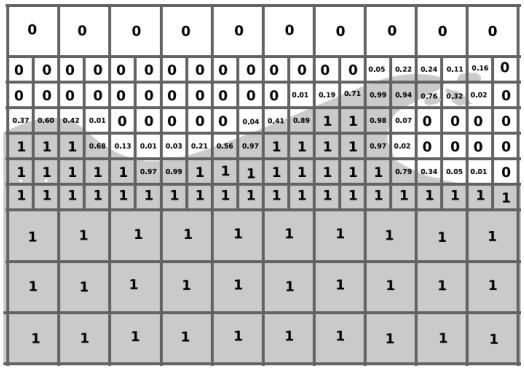

(a) *interFoam* and *interIsoFoam* (The VOF method)

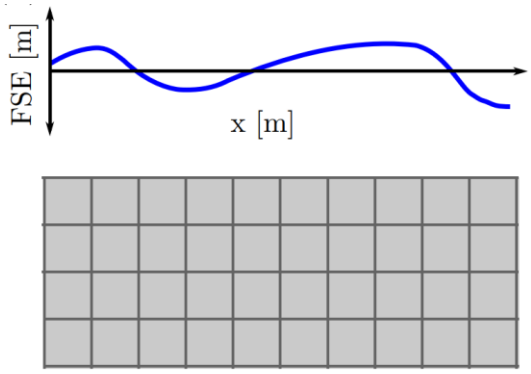

(b) *potentialFreeSurfaceFoam*

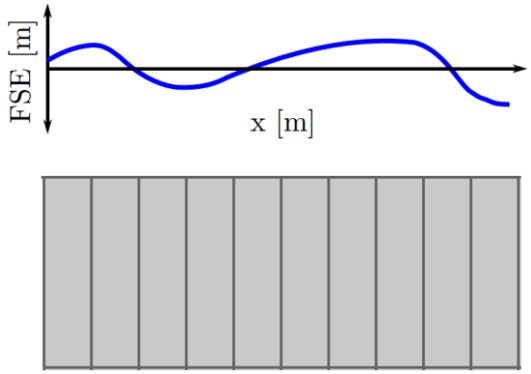

(c) *shallowWaterFoam*

Figure 3: Depiction of the methodologies of different OpenFOAM solvers for free-surface flow [22].

The most commonly used OpenFOAM solver for wave modelling is *interFoam*, which considers two fluid phases (air and water) and that the fluids are incompressible, immiscible, and viscous. However, other solvers, shown in Figure 3, might be more efficient for specific cases e.g. simulating an oil spill [23], or to include air compressibility e.g. calculating wave impact/slamming loads [24–26] and simulating an oscillating-water-column WEC [27,28]. In addition, it is possible to decrease the complexity of the model by neglecting the effect of viscosity e.g. to reduce the computational burden of fully resolving the boundary layers [29].

A variant of the *interFoam* solver, *interIsoFoam*, has been developed and is gaining popularity due to its improved ability to handle the free surface interface. The *interIsoFoam* solver employs the novel geometric VOF algorithm, *isoAdvector* [30], which maintains a sharp interface by constructing and advecting an isosurface inside the cells around the interface position. By contrast, the original *interFoam* solver utilises the multi-dimensional limiter for explicit solution (MULES) method, which employs an artificial compression velocity term to bound the interface [31]. Considering wave propagation, *interIsoFoam* has been shown to maintain a sharper interface than *interFoam* [32] and significantly reduce the excessive wave

dissipation inherent in traditional VOF methods [33], despite the considerably higher computational cost.

To tackle the spurious velocities and, thus, allow lager time steps and better performance of turbulence models at the interface, recently, the Ghost Fluid Method (GFM) has been implemented within OpenFOAM [34]. The GFM ensures a continuous velocity field across the interface by coupling the two phases (high and low density) via specific jump conditions at the interface.

In a comparative study, Peltonen et al. [35] investigated the performance of the GFM (based on [34]) and the traditional VOF for a number of marine-related test cases, i.e. two-dimensional inviscid flow over a step, two-dimensional interface shear layer, and ship wave generation for a Wigley hull and the Hamburg test case. The authors found rather subtle differences for the specific test cases and suggest a further improvement by coupling GFM with geometric interface capturing methods, such as *isoAdvector*.

Recently, MULES has been improved with the Piecewise-Linear Interface Calculation (PLIC) and Multicut PLIC (MPLIC) [36]. PLIC represents an interface by surface cuts that split each cell to match the volume fraction of the phase in that cell. The surface cuts are oriented according to the point field of the local phase fraction. The phase fraction on each cell face, i.e. the interpolated value, is then calculated from the amount submerged below the surface cut. MPLIC is for handling multiple surface cuts, where a single cut in one cell is insufficient, e.g. the water volume in one cell is between two separated air volumes. PLIC and MPLIC thus have improved the modelling of interface/free surface, e.g. achieved high-resolution modelling of water splash [37].

2.1.2 Alternative methods

Schmitt et al. [22] explored the choice of solvers in OpenFOAM other than those based on the VOF method, which could be utilised to implement numerical wave tanks, namely: *potentialFreeSurfaceFoam* and *shallowWaterFoam.* While hundreds of publications have utilised the VOF method for WSI, Schmitt et al. [22] found that less than a dozen have used *shallowWaterFoam* and only two have used *potentialFreeSurfaceFoam*.

The *potentialFreeSurfaceFoam* solver is a single-phase solver, as depicted in Figure 3(b), that calculates the free surface as a single-valued function, thus cannot simulate effects such as wave breaking. *PotentialFreeSurfaceFoam* is based on the *pimpleFoam* solver, which is widely used in a broad range of applications for incompressible, single-phase, transient flows. A special boundary condition is added to the *pimpleFoam* solver, called *waveSurfacePressure*, which

calculates the change in surface elevation at each time step based on the volume flux for the cells at the top boundary. The *shallowWaterFoam* solver employs simplified equations that are valid in shallow water conditions. The shallow water equations [38] enable the velocity to be represented by a depth-averaged horizontal component, eliminating the requirement to solve for the vertical direction. Therefore, massive reductions in the overall cell count are achieved since the domain only needs to be discretised using one cell in the vertical direction, as depicted in Figure 3(c). The shallow water equations only consider the water phase, thus *shallowWaterFoam* is a single-phase solver, where the surface elevation is directly available as a simulation variable. Another alternative solver is *interTrackFoam*, which applies an interface tracking that considers single-phase by enforcing the free surface boundary conditions on it [39]. However, this method is not applicable in a situation where the water can be discontinuous due to the structure, e.g. waves bring partial water to go on top of a structure [40], because in this scenario the free surface is no longer a continuous boundary. More examples of using alternative models to VOF can be found in Schmitt et al. [22].

2.2 Wave modelling

2.2.1 Variety of waves

There are a variety of wave theories that can be used to generate progressive ocean surface waves. The waves can be divided into regular (linear and nonlinear), irregular waves and focussed waves. In this sub-section, the implementation of different wave theories in OpenFOAM will be introduced.

For regular wave modelling the incident waves are periodic. To represent more realistic wave conditions, various regular waves of different wave heights and frequencies can propagate in a certain region, known as irregular waves (also sometimes called random waves). The spectrum of irregular waves can be obtained through on-site measurements and inputted into simulations. Commonly used wave spectra include the JONSWAP, the Pierson-Moskowitz and the Bretschneider types [41,42], in which JONSWAP is considered the most widely used.

Focussed waves are normally considered when assessing extreme wave loads, where a single high-crest wave is formed due to the accumulation of wave components (although there are also trough-focussed or focussed at any particular phase). The focussed crest waves are normally formed through the delicate superposition of multiple wave peaks.

When the water waves approach the coast, the water depth decreases to shallow enough that the wave may feel the presence of seabed and change its shape. This action induces increasing wave height and decreasing wavelength, which will cause the wave to break at a certain point.

This process is known as surf zone breaking waves, shown in Figure 4. The bathymetry will influence the wave breaking type from spilling, plunging, collapsing, or surging. The modelling of breaking waves is different from modelling non-breaking surface waves (for non-breaking waves potential-flow theory or a laminar model can be used).

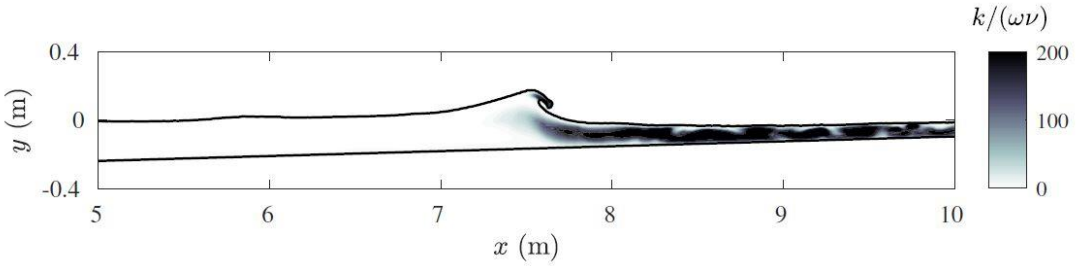

Figure 4: Plunging-type breaking wave simulation [43], where k/(ων) indicates the turbulence level.

In the deep-water regime of offshore/coastal regions, where the surface wave is not influenced by seabed, breaking waves can also occur due to the instability of wave trains subject to initially small perturbations. The resonant interaction between the carrier wave trains and the small perturbations can lead to an exponential growth of the wave amplitudes for the side bands, and further wave breaking. A study by Li and Fuhrman [44] simulated the so-called Class I (Benjamin-Feir instability) and Class II (crescent waves) deep-water wave instabilities involving wave breaking with the Reynolds stress turbulence model. Figure 5 shows the three-dimensional wave breaking evolved from crescent waves.

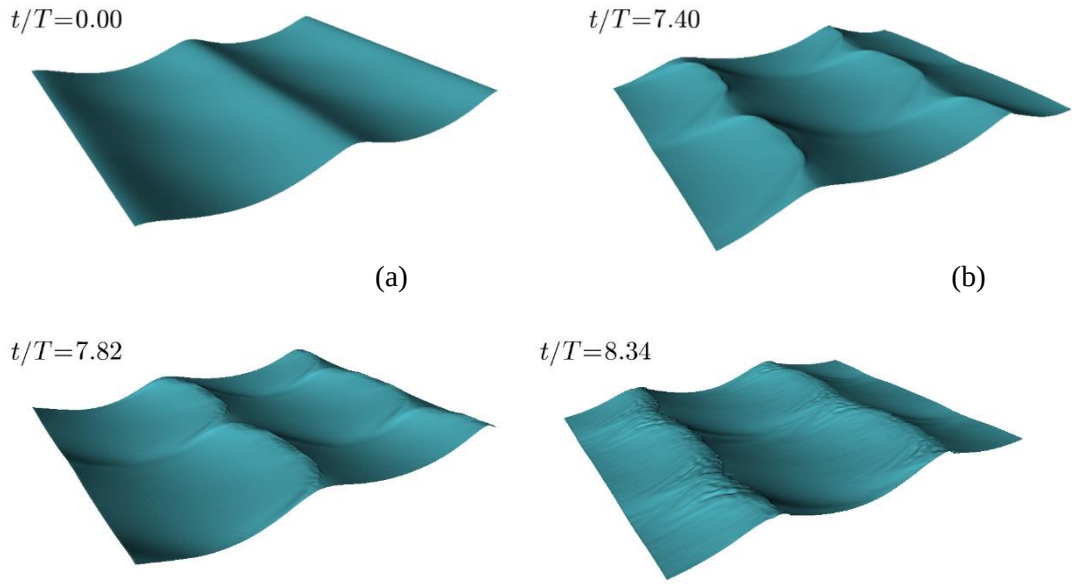

Figure 5: Free surface evolution during the interaction between a plane wave train and three-dimensional perturbations: (a) the initial 2D wave train (b) 3D crescent waves (c) wave breaking on the crescent crests (d) disturbed free surface during wave breaking [44].

In open seas, focussed wave groups can also form breaking waves. Resulting from the superposition of multiple waves or a storm, such rogue waves can be formed as a random event [45]. Bredmose and Jacobsen [46] modelled breaking waves generated from focused wave groups using the *interFoam* solver and investigated the breaking wave interaction with an offshore wind turbine foundation in the intermediate water. As strong turbulence is produced in wave breaking, this will require turbulence modelling that will be discussed in Section 2.2.3.

2.2.2 Wave generation and absorption in OpenFOAM

To model waves numerically, it is essential to consider the generation of the desired wave at the inlet of the Numerical Wave Tank (NWT) and the absorption at the outlet to avoid reflected waves. Numerical wavemakers can be implemented by different methods, namely: (a) including a physically similar wave generator/paddle by making the inlet boundary move - this method is similar to wave tank experiments [47,48]; (b) implementing dictating functions to force the CFD solutions to present a target wave condition, where the relaxation method and the static boundary method are two of the maturest [49,50]. For (a), additional boundary condition modifications and dynamic mesh treatment are required, therefore (b) is the typical approach is NWT modelling.

In the case of the relaxation technique, the generation of the wave is initialised by using the analytical solution of the wave theory applied in the inlet zone. Normally the solutions are also artificially changed in the outlet zone to absorb the wave thus modelling a far-field condition, as shown in Figure 6(a). This method has been implemented in a toolbox named *waves2Foam* [51].

In the relaxation approach, a user-defined function is introduced to modify the solution of a computational variable ξ (e.g. velocity or volume fraction of water) of each timestep by blending a target value, as $\xi = \chi\xi_{computed} + (1-\chi)\xi_{target}$, where χ is the relaxation coefficient taking values between 0 and 1, as shown in Figure 6(b). With this method applied, theoretical target waves are forced at the inlet and outlet boundaries (where $\chi = 0$) and unmodified computed results are obtained in the middle of the NWT, where $\chi = 1$, with the inlet and outlet zones gradually changing χ to relax the solution change. The relaxation technique has been proven effective and stable, mostly able to generate and absorb waves with negligible error [52–54]. Nonetheless, the size of the computational domain tends to increase due to adding the relaxation zones.

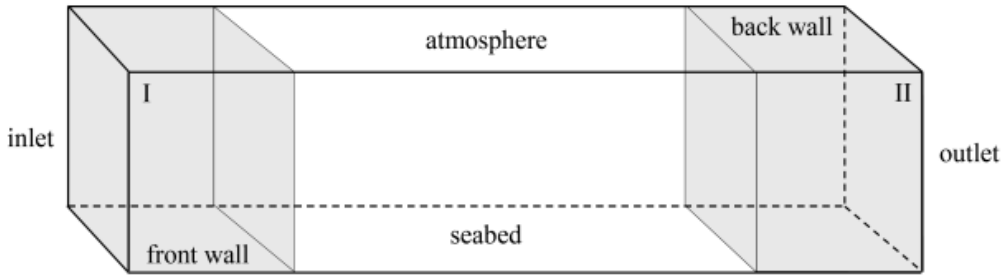

(a) Inlet and outlet relaxation zones (grey) in a numerical wave tank

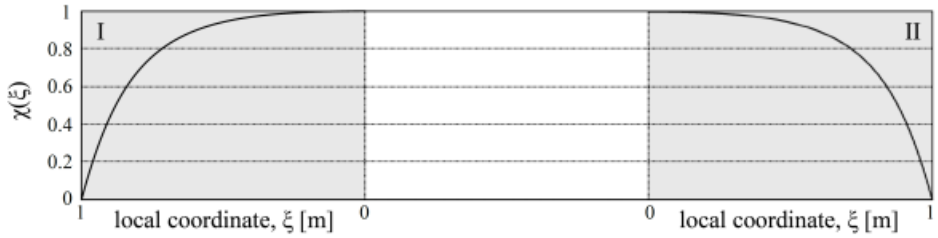

(b) The value of the spatial weighting factor

Figure 6: Illustration of the relaxation method [55].

As an alternative, the static boundary method that uses boundary conditions to control the generated wave was developed, and it is available in OpenFOAM as *IHFoam* and *olaFlow*

[10,56]. At the wave generation boundary, the boundary conditions are obtained from wave theory. For the absorption boundary, a correction velocity is applied to cancel out the incoming waves. This method has also been successfully used across the WSI community [57–59], and further information on the developer's toolbox can be found in [51,60,61].

Compared to the relaxation method, the static boundary method can avoid the use of relaxation zones that increases the computational cost. Nonetheless, it has been highlighted that wave absorption using the static boundary method is a challenge. The wave field near the outlet boundary is normally disturbed by a structure, i.e. it is not pre-known as an incident wave field, so measuring the flow before the outlet is essential for the cancelling out. However, the measured flow near the outlet is a combination of incident and reflected wave, which means wave filters must be used to derive a cancelling-out wave train from the outlet. The wave filtering technique strongly relies on wave theories. Previously, this approach was only valid for linear wave theory in shallow water [62]. Further development has been made by Higuera [63] to enable the absorption of deep waters, but the author still highlighted the incapability of absorbing nonlinear waves. Recently, Borsboom and Jacobsen [64] have made an advancement by analytically decomposing the measured flow into multiple modes. This significantly improved the absorption of nonlinear waves and the undesired reflection was reported to be less than 5% of the incident waves.

Windt et al. [65] used different test cases to assess available OpenFOAM methods for numerical wave tanks. Their comparison suggested that the static boundary method is the most computationally efficient for wave generation, while the wave absorption part may be better replaced by using a numerical beach method, which is implemented as a dissipating region nearby the outlet.

For either the relaxation method or the static boundary method, it is worthwhile to note that at least 10 cells per wave height and 100 cells per wavelength should be used to generate an accurate target wave. This mesh density generally gives a deviation of less than 1% against theoretical waves, provided that other setups are reasonable [66]. More information on the different wave generation methodologies can be found in the reviews of Schmitt and Elsaesser [67], and Windt et al. [68].

2.2.3 Turbulence modelling

WSI can be accompanied by significant turbulent behaviours that dissipate the kinetic energy and change the fluid behaviours and structural loads. Direct Numerical Simulation (DNS) can accurately replicate turbulent flows, but this requires solving the Navier-Stokes equations with

an extremely high mesh density that most computing facilities can unlikely afford. As a result, assumption-based modelling is commonly required. Such assumptions have categorised turbulence modelling strategies into several groups, known as Reynolds-Average Navier-Stokes equations (RANS), Large-Eddy Simulation (LES) and their combination (Hybrid). These methods apply certain numerical treatments to account for the turbulent effects in the simulation, allowing savings in cell amount. More details of different turbulence modelling approaches can be seen in [69]. Figure 7 illustrates the approaches' levels of fidelity and the computational demand.

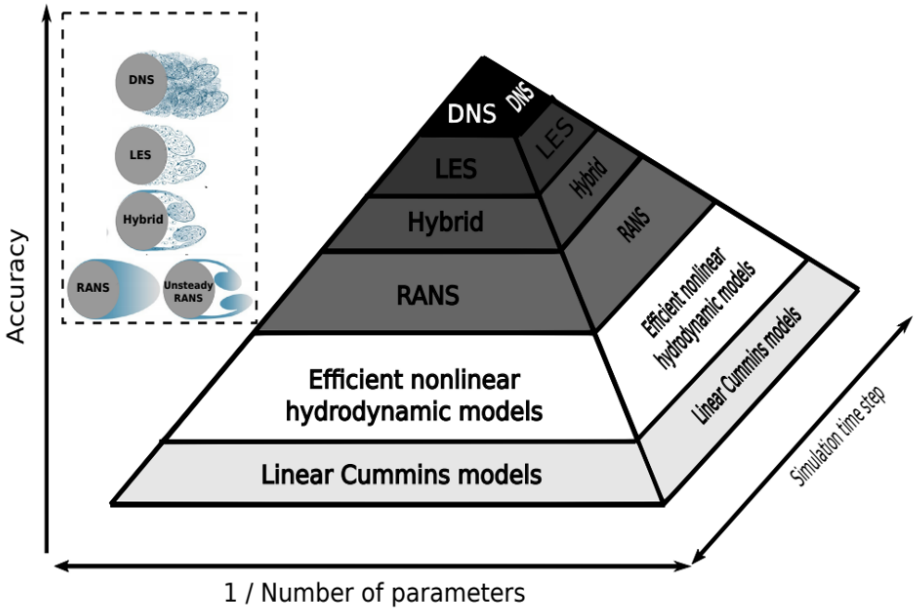

Figure 7: Illustration of the fidelity and computational requirement for different turbulence modelling methods [70].

In general, most of the studies of WSI have employed a two-equation model, e.g. the k-ω or k-ε model (where k is the turbulence kinetic energy, ω is the specific dissipation rate and ε is the dissipation rate of turbulence) to close the RANS equations for the turbulent flow [71]. This can be corroborated by Windt et al. [72] on the modelling of WEC (Figure 8). Besides two-equation models, there are also other RANS-based turbulence models, e.g. Algebraic models, one-equation models, Reynolds stress models (RSM). There are two main reasons for RANS-based two-equation models to be the mainstream choice: (a) the computational resources required for RANS-based two-equation models are much lower than Hybrid or LES, which makes RANS simulations mostly affordable by contemporary computing facilities. (b) RANS-based two-equation models are seen to provide sufficient accuracy for many 3D WSI

applications, so there is normally no necessity to apply a higher-order turbulence modelling approach. Validation examples of RANS-based turbulence modelling in various WSI applications will be presented in Section 3.

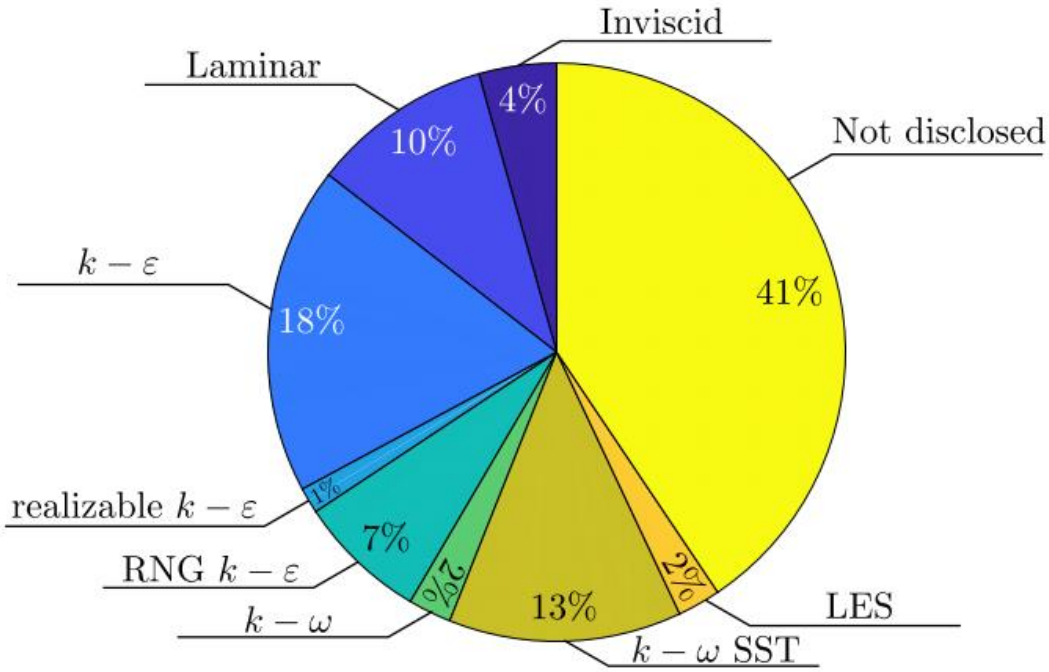

Figure 8: Turbulence models used for CFD modelling of wave energy converters [72].

Two-equation turbulence models have also been widely used in the past two decades for simulating surf zone breaking waves. However, seemingly all the simulations with two-equation models (both *k-ω* and *k-ε* types) have shown a tendency to overestimate turbulence levels for breaking waves, both in the pre- and post-breaking regions. For example, the results presented in Brown et al. [75] performed with OpenFOAM using different turbulence models have shown over-production of turbulence even in the pre-breaking regions (in this region, the waves can be modelled with potential-flow theory and the turbulence is nearly zero). The same phenomenon has also been observed in the simulations by Devolder et al. [76] who added buoyancy production terms to the *k-ω* branches to eliminate turbulence pollution from the air to the water phase.

Recently, Larsen and Fuhrman [77] have proved that this problem is due to the unconditional instability of two-equation turbulence closure models (both k-ω and k-ε types) in the potential flow core region beneath surface waves. A method for formally stabilising two-equation models was derived in their work, and it was shown that stabilised two-equation models lead to

pronounced improvement in the predicted turbulence and undertow velocity profiles prior to breaking and in the outer surf zone. Fuhrman and Li [74] analysed a more complicated but popular turbulence model – the realizable k-ε model. They found that this model is conditionally unstable in the potential flow region beneath surface waves. They likewise stabilized the realizable k-ε model so that the initial conditions would not affect the stability (without exponential growth of turbulence beneath waves in the potential flow region). However, even the stabilized two-equation models in Larsen and Fuhrman [77] and Fuhrman and Li [74] were still rather inaccurate in the inner surf zone (i.e. closer to the shoreline), thus seemingly requiring yet more advanced methods of achieving turbulence closure.

Li et al. [43] analysed more advanced RANS-based Reynolds stress turbulence models (RSMs) which solve all components of the Reynolds stress and break free from the Boussinesq approximation (which is a basis for all RANS-based two-equation models). The RSMs were proved to be reasonable for simulating non-breaking progressive wave trains without having the problem of over-production of turbulence in the potential flow region beneath surface waves. The RSM model has also achieved good accuracy in the prediction of coastal breaking waves on a sloping beach, especially the undertow velocity, as presented in the work of Li et al. [43,73]. The model has also been applied to simulate the deep-water wave instabilities involving wave breaking, as presented in Li and Fuhrman [44]. The RSM model in terms of the stress-ω model is publicly shared through Li [78].

Nonetheless, some WSI studies performed with the laminar model (assuming no turbulence effect) have also shown good accuracy, e.g. [79]. This is probably due to the fact that the waves are non-breaking and the inertial effect in the problem is stronger than the viscous effect. Therefore, whether turbulence modelling is required for solving a WSI problem depends on the physics of the fluid flow in the particular case. For example, Li et al. [79] examined the Keulegan-Carpenter (KC) number for their study case on waves interaction with a gravity-based foundation. They found that the turbulence effect is negligible as the KC number is relatively low, in which case a turbulence modelling approach may not be used.

2.2.4 Air entrainment

Air entrainment can be driven by turbulent motion near the free surface e.g. high-velocity open channel flows. High-fidelity studies such as DNS have been conducted on air entrainment in relatively small-scale problems such as in the case of a stationary turbulent hydraulic jump [80]. For larger-scale problems such as spillways, DNS is less practical due to the vast computational cost. Rather, RANS turbulence models have been widely applied. For example, Lopes et al. [81] implemented the entrained air flux estimator of Ma et al. [82] in *interFoam*, coupled with

the k-ω SST turbulence model to simulate the stepped spillway.

Air entrainment is also commonly considered in breaking waves. Tomaselli [83] numerically investigated the air entrainment in breaking waves and their interaction with a monopole also using *interFoam*, combined with an LES turbulence approach. The air phases in the aforementioned studies were considered incompressible. Air compressibility has also been considered and implemented in OpenFOAM as *compressibleInterFoam*. Relevant studies can be found such as Ferrer et al. [26] and López et al. [28] who studied dam break, plunging wave impact at a vertical wall, and an oscillating water column.

3. WSI modelling

3.1 Wave interaction with rigid fixed structures

Wave interactions with rigid fixed structures are one-way processes and are commonly seen in coastal defence and offshore wind turbines. Figure 9 provides an example of this type of WSI. As the structure is fixed, the modelling contains the least computational challenge compared with those to be introduced in the next sections. This is because the fixed structure can be treated as a wall boundary condition that does not involve any structural solutions or dynamic mesh treatment. Therefore, successful modelling for this type of WSI mainly relies on accurate representation of the fluid behaviours, i.e. the wave or turbulence modelling, which has been introduced in Section 2.

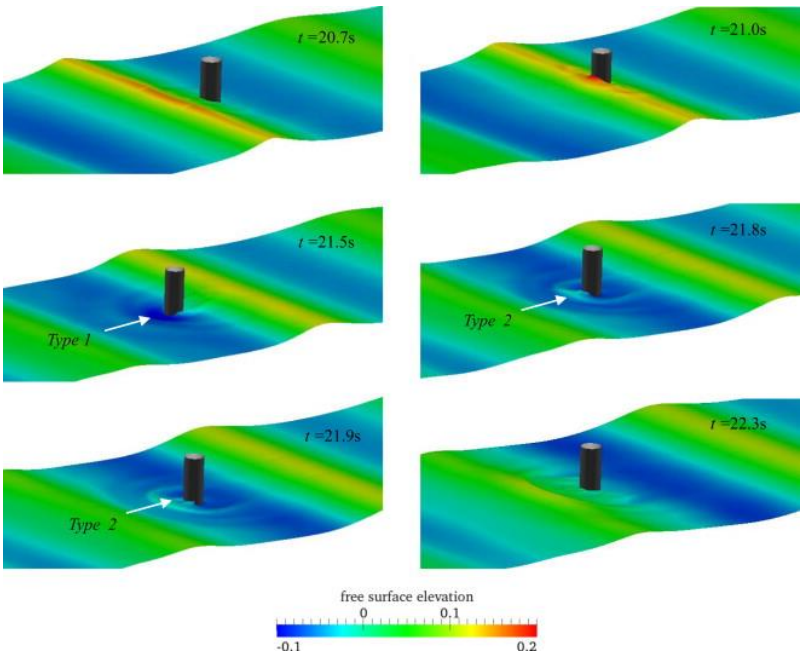

Figure 9: Uni-directional waves interacting with a fixed cylinder [41]

Extensive studies have used OpenFOAM to assess coastal and offshore engineering problems with a fixed structure. Since a sea wall or a breakwater normally expands extensively in the profile direction, 2D simulations have been widely used to perform analyses and agree well with wave flume experiments. For example, Morgan and Zan [84] demonstrated OpenFOAM's ability to produce accurate results for a wide variety of 2D wave conditions and geometries. They considered submerged breakwater cases where it was found that the numerical predictions agree with the experimental data, in terms of waveforms and wave amplitude spectra. Their setup can be used to investigate the dependence of the wave transmission and reflection properties of the breakwater. Chen et al. [85] performed 2D simulations to predict wave overtopping on a dike structure. Their prediction of overtopping water level agrees with the experimental measurements in the time domain. However, the accuracy is based on a stabilised k-ω model developed by Larsen and Fuhrman [77], which is essential for accurately modelling wave propagation in the coastal region and breaking on a structure.

In order to account for 3D structures in uni-directional waves but avoid the computational cost of modelling a whole computational domain in 3D, a 2D-3D coupling model was developed by Di Paolo et al. [86,87], where 2D was used to solve wave generation from the inlet, stable propagation towards the structure, and absorption near the outlet; 3D was used only around the structure. Validation against experimental data demonstrated that this approach can provide accurate predictions when considering uni-directional wave conditions.

Full 3D simulations are required for the 3D multi-directional wave conditions as in real sea states. However, the wave modelling may be simplified by the spectral approach, which provides boundary conditions for a small CFD computational domain near the structure. An example of this treatment is HOS-NWT [88], which has been validated against experiments [89]. Decorte et al. [90] used the HOS-NWT approach to assess the wave load on a fixed wind turbine, according to the statistics in non-Gaussian seas.

3.2 Wave interaction with rigid floating structures

The interaction of waves with a rigid floating body is a two-way process. Waves can induce body motions, and meanwhile those motions change the surrounding wave field. An example is shown in Figure 10. To model this type of problem, one of the multiphase solvers of OpenFOAM is needed to be used, e.g. *interFoam*. However, as the floating body is moving, simulations need to be carried out with dynamic mesh. The particular module for dynamic mesh can be *sixDoFRigidBodyMotion*. This module enables us to model the six degrees of freedom motion under the action of fluid and body forces. The motions in different directions can be restrained. In summary, *sixDoFRigidBodyMotion* is used for wave-induced motions. In another

scenario where the body motion is prescribed rather than induced, another module called *solidBody* may be used. *solidBody* allows to model either prescribed linear or angular harmonic motions. Such motions might help to model the radiation problem from the prescribed motions of a floating object. Simulating prescribed harmonic motions can also help measure the hydrodynamic coefficients of a floating object.

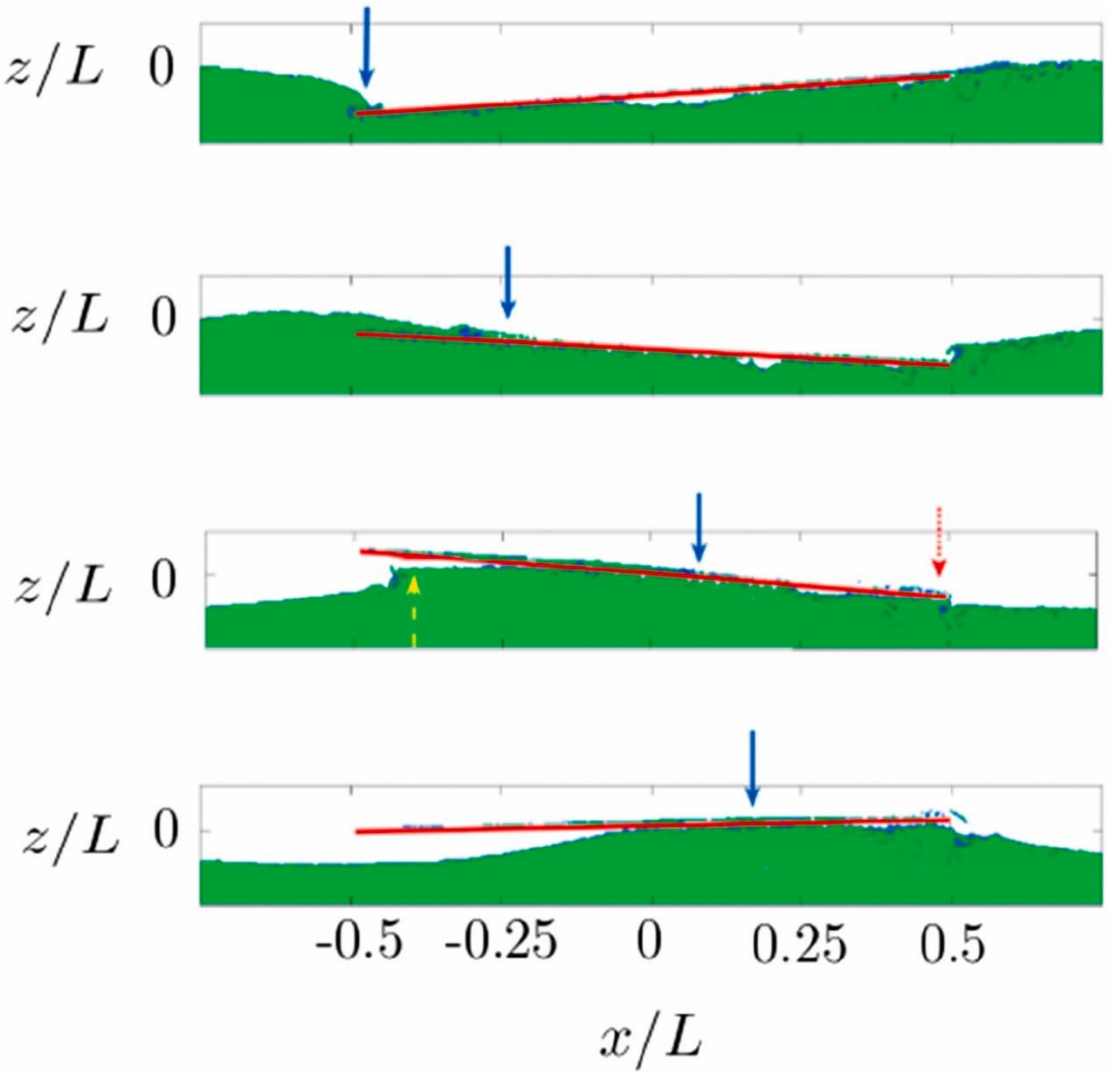

Figure 10: Wave interaction with a rigid floating plate [91]

The main challenge in modelling the dynamic motion of an object is the way the mesh motion is handled. Two different methods can be used for six-degree-of-freedom simulations: *dynamicMotionSolverFvMesh* and *dynamicOversetFvMesh*, known as the morphing-mesh method and the overset method.

dynamicMotionSolverFvMesh morphs the mesh over every time step, where there are different libraries for single-body, *sixdofrigidbodymotion*, and for multi-body, *rigidbodymotion*. The

number of cells in the meshing methodology is not changed over time, but the cells might get distorted or flexed under the action of the motion of the solid body. An inner and an outer distance around the body are identified. The changes in the cells occur in the area located in between these two distances. When the motion of the solid body moving under the action of forces is relatively large, simulations might crash. This commonly happens due to large distortion of the cells, which needs to be treated by additional steps, such as reconfiguring the mesh after a certain simulation duration, sliding the mesh, or adding a dedicated motion interpolating scheme [40,92,93].

Extensive work has been carried out by using the morphing technique. In Palm et al. [94], CFD simulations were performed to model the dynamic response of an ocean WEC exposed to other waves. In Islam et al. [95], CFD simulations were run to numerically replicate the wave-induced motion of a floating barge exposed to water waves. More examples of the morphing-mesh technique in WSI can be found in [59,96–98].

dynamicOversetFvMesh, known as the overset approach, divides the computational mesh into two parts: background mesh and overset mesh (where multiple overset regions are possible). The background mesh denotes the fluid domain which is a fixed Eulerian framework; while the overset mesh attaches to the structure, moving together with the structure based on its Lagrangian framework. In this way, both parts of the mesh are not distorted. This method is particularly used for cases with large motions to overcome the limitations of the *dynamicMotionSolverFvMesh* for those cases, such as a swinging WEC, large structural motions induced by rogue waves, planning hulls, or a water-entry process [45,99,100]. At the present stage, the *overInterDyMFoam* solver is used for overset simulations. The application of the *overset* method for wave-structure interaction problems is well documented in [101]. The main challenge of overset, however, is inaccuracies resulting from the interpolation that is needed to couple the background and overset regions. Due to this, *overset* may violate mass conservation, and the pressure equation needs to be adjusted implicitly to guarantee the transfer of fluxes correctly between overlapping regions. Corresponding mitigations may be seen in [102]. Another potential solution is to build the overset region sufficiently large to avoid communication locations near the area of interest [100], i.e. farther from the structure, which might help in predicting the fluid load/impact.

Simulations using the overset technique for WSI are also widely conducted. Wu et al. [103] simulated the dynamic motion of small floating bodies, which may resemble solitary small ice floes. They used the overset technique to model different geometries of ice floes. They successfully modelled the wave-induced drift motion of ice floes, having oscillatory motions in all six degrees of freedom. The model was found to have a great level of accuracy in the

prediction of the motion, following validation against experiments. Benites et al. [99] have used the overset technique to model a WEC rotating with a large angle, and good agreement with experiments was reported. A power-take-off model is incorporated into the motion solver as a spring-damping effect. Other overset applications in WSI can be found in [91,104,105].

3.3 Wave interaction with deformable structures

WSI can also involve a deforming structure. For example, flexible wave energy converters that deform with waves are shown to have higher efficiency and lower structural risk than rigid ones [106]; deforming breakwaters demonstrate evidently better wave-attenuation performance than rigid ones [107]; natural features such as sea ice and vegetations also can deform with waves [108,109]. To include the deformation significantly increases the computational challenge, because CFD itself does not contain structural deformation. Therefore, CFD is required to be coupled with an additional set of computational solid mechanics (CSM) equations to calculate the structural deformation. If the CSM solution is not fed back to CFD, this mechanism is known as one-way coupling, and this is commonly applied for stress analyses, where the solid deformation is inconspicuous while the structural internal stress can be critical, e.g. [110]. However, for WSI processes, deforming structures may also significantly change the surrounding fluid field, if the structural deformation is large. In order to accurately simulate the fluid field, the CSM solution is required to be fed back to CFD to enable a two-way Fluid-Structure Interaction (FSI) process.

Waves' interactions with flexible vegetation such as seagrass have also been simulated using OpenFOAM. Chen et al. [111] presented a coupled wave-vegetation interaction model for simulating flexible vegetation such as seagrass. The wave hydrodynamics is modelled with *IHFoam*, and the vegetation motion is solved with the finite element method. The wave and vegetation models are coupled with an immersed boundary method. The above work used a combination of solvers, e.g. *interFoam* for CFD and an external solver for CSM, which requires a third code for coupling, data interpolation and simulation management. This usually results in the FSI being one-way coupling, thus not fully representing the physics.

The realisation of a two-way coupling FSI simulation can be achieved through a partitioned approach. For every time step of the FSI simulation, (i) the solution of the fluid part is obtained first, and then the fluid solution is passed as a force on the fluid-solid interface, so that the solid part can solve the solid deformation. (ii) The deformed solid mesh will also induce the fluid mesh to deform. In weakly coupled FSI, the solver goes to the next timestep immediately after step (ii), i.e. without further iterations between fluid and solid domains. This may be acceptable when the solid deformation is small, as the influence of mesh deformation on the fluid velocity

field can be negligible. However, when the solid deformation is large, weakly coupled FSI will induce errors i.e. inconsistent dynamic and kinematic features between fluid and solid at the interface, and the errors can be accumulated over each timestep, leading to unreliable results. To enable a strongly or fully coupled FSI, after step (ii), the fluid solution (i.e. velocity and pressure of the fluid domain) is updated again in the current timestep, because the fluid domain has changed with the mesh deformation. If the fluid part is solved again, likewise, the solid solution will need to be updated again. This can require a large number of iterations until the fluid and solid parts are fully coupled, i.e. with consistent dynamic and kinematic features at the interface), while this demonstrates a higher level of accuracy than one-way coupling or weakly two-way coupling. Such a process that solves fluid and solid separately is therefore called a partitioned approach. Fluid and solid can also be implicitly solved together, but this FSI approach is still under development in OpenFOAM, with some early progress shown, such as [112–114].

Based on the partitioned approach, OpenFOAM has made substantial progress in terms of FSI simulations. Tukovic et al. [115,116] developed an FSI code based on OpenFOAM (*fsiFoam* solver) with strong two-way coupling as introduced above. An advantage of this OpenFOAM approach is that it employs the finite-volume method (FVM) for both fluid and solid domains [115,117]. Most current FSI works involve a combination of solvers, usually with a finite-volume solver for the fluid flow and a finite-element solver for the structural analysis, e.g. [118], which requires a third code for coupling, data interpolation and simulation management. Thus, the combined alternative approaches for the fluid and solid domains will tend to increase computational costs and imposes limitations on the coupling method. In contrast, the entirely FVM approach of Tukovic et al. [116] makes an all-in-one solver under the framework of OpenFOAM.

One limitation of *fsiFoam* was that it could only be applied to single-phase fluid modelling. Therefore, it could not be used for multi-phase applications, e.g. WSI containing both air and water. In order to simulate hydroelastic problems within OpenFOAM, Huang et al. [119] incorporated *fsiFoam* with the VOF approach to model multiphase flows, furtherly, with *waves2foam* to model WSI (named *waveFsiFoam*). In this way, simulations were enabled for hydroelastic interactions of waves with a large elastic ice sheet [108] and with an elastic breakwater [107], and the accuracy was validated against experiments. Figure 11 gives an example of highly-nonlinear breaking waves interacting with a seawall that undertakes large deformations.

In recent years, the development of *fsiFoam* has been combined with a FSI toolbox, *solids4foam*, led by Cardiff et al. [120]. *solids4foam* has made a significant advancement particularly in

structural solutions, by enabling the FSI simulations of viscoelastic, thermoelastic, and poroelastic solids [120,121]. *solids4foam* is currently deemed to be a long-term FSI framework of the OpenFOAM family and a robust solver for structural analyses. More applications of *solids4foam* can be found in [122–124].

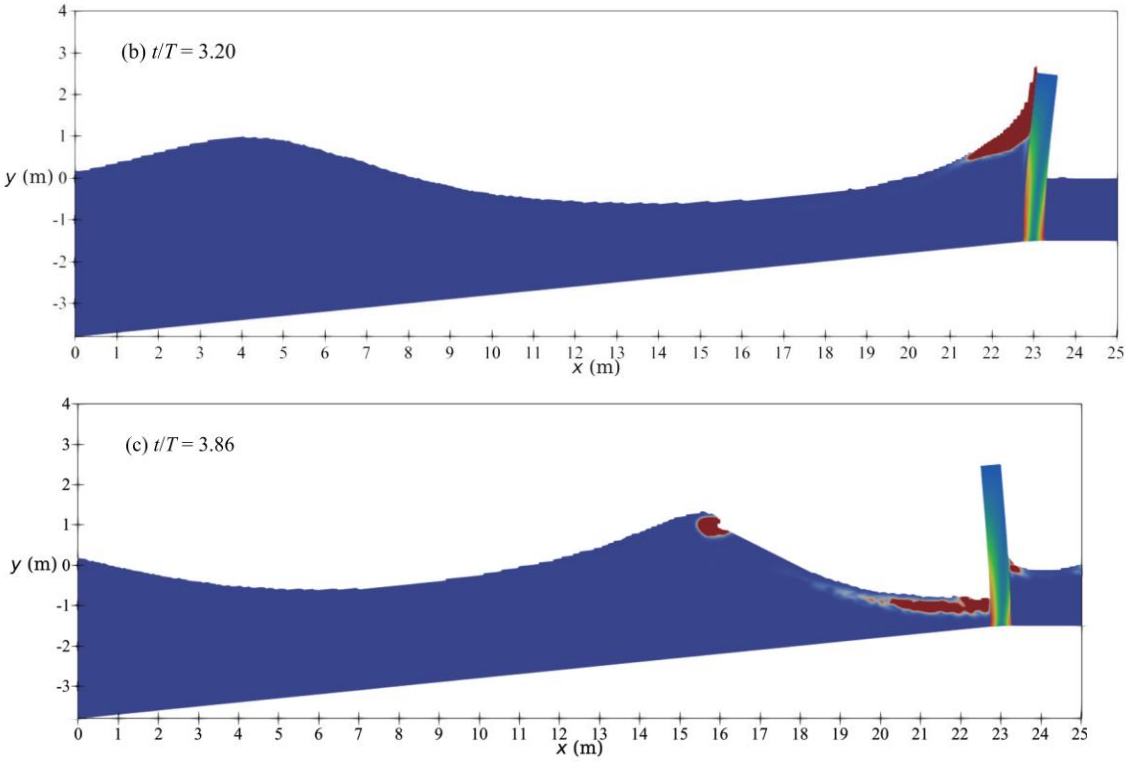

Figure 11: An elastic seawall hit by highly nonlinear breaking waves [125]

3.4 Wave interaction with porous structures

The two main methods to model wave interaction with porous structures are the micro- and the macro-scale approaches. With the micro-scale approach, the detailed geometry of the structure is resolved explicitly. This allows for high-fidelity investigations of the FSI. Accurate geometry and fluid flow resolution, however, require a large number of mesh cells, and thus, a high computational demand. With the macro-scale approach, the effect of the porous structure on the fluid is applied by means of its bulk effects. Here, the porous structure is not explicitly resolved but represented by a geometrically defined porous region in which a volume-averaged macro-scale model is added to the momentum equation through a source term. This approach cannot reproduce the exact fluid flow inside or close to a porous structure but can provide a sufficiently accurate replication of the mean flow for many WSI problems. The advantage of this approach is a smaller computational demand due to the smaller number of mesh cells

637 required. A comprehensive review on the mathematical foundations and solution techniques of
638 macro-scale approaches in the context of coastal structures is given in Losada et al. [126].

639 Porous structures can be categorized into large volumetric structures such as breakwaters or
640 vegetation, and thin porous structures such as perforated or slotted barriers. Depending on the
641 overall aim of the simulation, either the micro- or the macro-scale approach can be more
642 suitable. For thin porous structures, the micro-scale approach has been used in most of the
643 literature, where common objectives are to derive hydrodynamic coefficients, as for instance
644 by Mentzoni and Kristiansen [127] for an oscillating perforated sheet or by George and Cho
645 [128] for a sloshing tank with a baffle; or to validate simpler (e.g. analytical) models, as for
646 example by Poguluri and Cho [129] for a vertically slatted barrier. Conversely, the macro-scale
647 approach has mainly been applied for thin porous structures when it is challenging to
648 geometrically resolve the structure or when the overall forces are of interest rather than details
649 of the flow. Examples are studies on fluid interaction with fish cages by Shim et al. [130] and
650 Chen and Christensen [131] and with circularly perforated structures by Feichtner et al. [132].
651 For large volumetric structures, it is common to use a macro-scale approach when the bulk
652 effects are to be investigated. This avoids challenges in resolving the often complex and
653 irregular geometries of the structures, and reduces the computational demand significantly
654 whilst providing sufficiently accurate fluid flow replication. Examples are simulations of wave
655 interaction with breakwaters by Jensen et al. [133] and Higuera et al. [134,135], or with
656 vegetation, for instance by Hadadpour et al. [133]. In contrast though, Maza et al. [136]
657 represented a mangrove forest microscopically by means of a cylinder array and studied
658 tsunami wave interaction.

659 Within a macro-scale approach, the general formulation of the pressure drop across a porous
660 structure, commonly called the extended Darcy-Forchheimer law, $\frac{\Delta p}{x} = au + \frac{b}{2}u|u| + c\frac{\partial u}{\partial x}$,
661 where a, b and c are porosity coefficients that are added to the momentum equation to account
662 for the effect of the porous structure on the fluid. The linear term represents viscous effects,
663 dominant for flow regimes with small Re-numbers; the quadratic term represents turbulent
664 effects with large Re-numbers; the transient term represents effects due to fluid flow
665 acceleration across the porous voids. The relative importance of the viscous, inertial and
666 transient terms and the related formulations of the porosity coefficients (a, b, c) are highly
667 problem-specific and key to accurately representing the properties of the structure and the
668 corresponding flow regime. For applications to volumetric granular material of coastal
669 structures, options of formulations are provided in the review by Losada et al. [126]. A
670 comparison of common formulations for the drag coefficient, b, for slatted barriers can be found
671 in the work by Poguluri and Cho [129].

672 The porous pressure-drop equation can be implemented in three ways. One option is the
673 implementation of volumetric porous media with either isotropic or anisotropic characteristics.
674 This works for both thin and large structures. An additional option for thin structures with
675 negligible thicknesses, is the porous baffle implementation where a pressure drop is applied
676 across a surface. An overview of the different types of implementation including illustrations
677 can be found in Feichtner et al. [137], where the three types have been compared for simulations
678 of wave interaction with thin perforated sheets and cylinders. The porous baffle or pressure-
679 jump condition is a standard implementation in OpenFOAM and can be used with *interFoam*
680 or any other application solver. It introduces the linear and quadratic term of the formulation in
681 the pressure-drop equation but neglects the transient term, and the input requires the thickness
682 of the porous structure and the coefficients a and b (in OpenFOAM referred to as D and F for
683 "Darcy" and "Forchheimer"). There was a porosity solver for two-phase flow named
684 *porousInterFoam* but this did not account for the limited amount of fluid inside the porous
685 structure which can lead to mass conservation problems. This deficit was for instance addressed
686 by Jensen et al. [138] and Higuera et al. [134] who implemented macro-scale porosity based on
687 the volume-averaged RANS (VARANS) equations, in combination with the wave modelling
688 toolboxes *waves2Foam* [139] (with the *porousWavesFoam* solver by Jensen et al., [138]) and
689 *OlaFlow/IHFoam* [134,135]. Both use porosity coefficients (a, b, c) based on granular material
690 by default but it is straightforward to transfer the input to also model thin porous structures, as
691 in Feichtner et al. [140,137]. Figure 12 provides an example of the macro-scale simulation
692 approach.

693

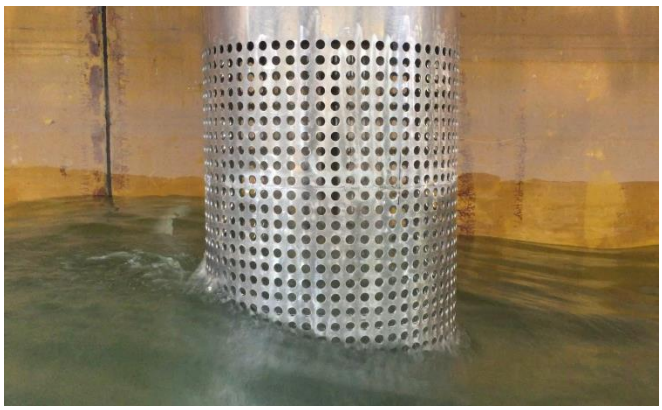

694

695 (a) The actual geometry

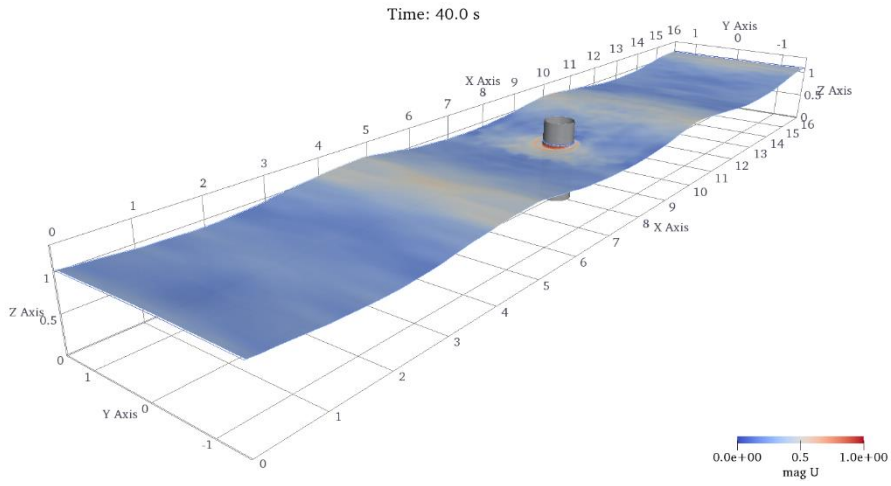

(b) Simulation

Figure 12: Wave interaction with a porous structure (macro-scale approach) [141]

A typical benchmark problem for fluid flow across a porous medium but without wave interaction is the 2D porous dam-break problem. Also Jensen et al. [138] and Higuera et al. [135] have used it for the validation of their porosity solvers where they followed the setups by Lin [142] and Liu et al. [143]. Additional examples of CFD modelling for wave interaction with microscopically resolved porous structures are works by Wu and Hsiao [144] on solitary wave interaction with a submerged slotted barrier, and by Lee et al. [145] on wave interaction with a circular perforated caisson breakwater. Further examples of wave interaction with porous structures represented by their macro-scale effects are studies by Srineash et al. [146] in the context of dams, by Brito et al. [147] on submerged vegetated floodplains and work by Zhao et al. [148] on a vertical net panel.

In the case of micro-scale porosity modelling, the challenges lie in the accurate representation of the geometry of the structure, the correspondingly large number of mesh cells that are required and the relatively high computational demand that follows as a consequence. The biggest challenge with the macro-scale approach is that the pressure-drop model and the formulation of the porosity coefficients (a, b, c) respectively are highly application dependent. Since no universal formulation exists, the models rely on coefficients derived from experiments or high-fidelity micro-scale models. The solution of a specific engineering problem in the context of wave interaction with porous structures generally requires a combination of experiments, simpler models, and models with higher fidelity. Another topic, where further studies are required, is that of turbulence modelling for macro-scale porosity representations. Opinions differ on whether a model is required at all or whether turbulence effects are already accounted for by the pressure-drop formulation. Losada et al. [126] provide a useful overview

of the viewpoints and arguments. They also identify future research needing to be done to answer the unresolved problems.

Maza et al. [136] used *IHFoam* to investigate tsunami wave interaction with mangrove forests. They compared two different conceptual approaches to model the mangrove forests: one is to directly simulate the detailed geometries of the rigid cylinder array; the other way is to consider the mangrove forests as a porous rigid media and apply volume-averaging to model the momentum damping created by the plants. The second approach can be more efficient; however, it was found that the maximum wave-exerted forces were underestimated.

3.5 WSI with seabed response

For offshore and coastal structures that are built upon the seabed, the investigation of the interaction between waves, the structure and the soil is critical for preventing future structure failures. In conventional geotechnical wave-soil interaction modelling, analytical wave pressure fields derived from linear or higher-order wave theories are usually applied as an external force for solving soil responses. However, the analytical solutions are often not accurate or not applicable to predict the wave-induced seabed responses in the presence of marine structures. When marine structures with complicated geometries are installed above the seabed, it will alter the wave field and the forces on the surrounding seabed. In order to achieve better predictions for wave-structure-seabed interaction problems, multi-physics numerical models have been developed, where the interaction between nonlinear waves and soil (in the presence of the structure or not) is modelled.

Liu et al. [149] made the first effort to investigate the seabed response in waves using an integrated CFD approach. They applied a solver in the OpenFOAM framework for two immiscible incompressible fluids (water and air) to produce a wave field with free surface. They also implemented a poro-elastic soil solver by discretizing the Biot's equations [150] for modelling the seabed. Later, Tang and Johannesson [151] extended their work into an anisotropic model in the quasi-static form in the OpenFOAM framework. The quasi-static anisotropic poro-elastic solver by Tang and Johannesson [151] was also validated and applied in the work of Li et al. [79] in which the anisotropic consideration was proven to be practical for modelling the seabed of medium and coarse sand. Li et al. [152] further developed the soil model in the partial-dynamic form and incorporated a liquefaction module considering different liquefaction criteria. The model is opensource at [78], and an example simulation is shown in Figure 13. Lin et al. [153] used this approach to investigate the nonlinear wave-induced seabed response around mono-pile foundation. Celli et al. [154,155] studied the effect of a submerged berm on the liquefaction near a rubble mound breakwater in regular and irregular waves. Liang

et al. [156] studied seafloor liquefaction around a pipeline under combined JONSWAP wave spectrum and current conditions. A variation of the poro-elastic model has been used by Ye et al. [157] to predict the subsidence of a rubble mound breakwater that exists in real life.

Plasticity modelling of the soil in OpenFOAM is also seen in the literature. Tang et al. [121] implemented an FVM-based code of poro-elasto-plasticity soil model. The model was built based on the Biot's consolidation theory and combined with a perfect plasticity Mohr-Coulomb constitutive relation. Elsafti and Oumeraci [158] implemented a multi-yield surface plasticity model to simulate plastic soil response under cyclic loads in their CFD solver geotechFoam, also developed in the OpenFOAM framework.

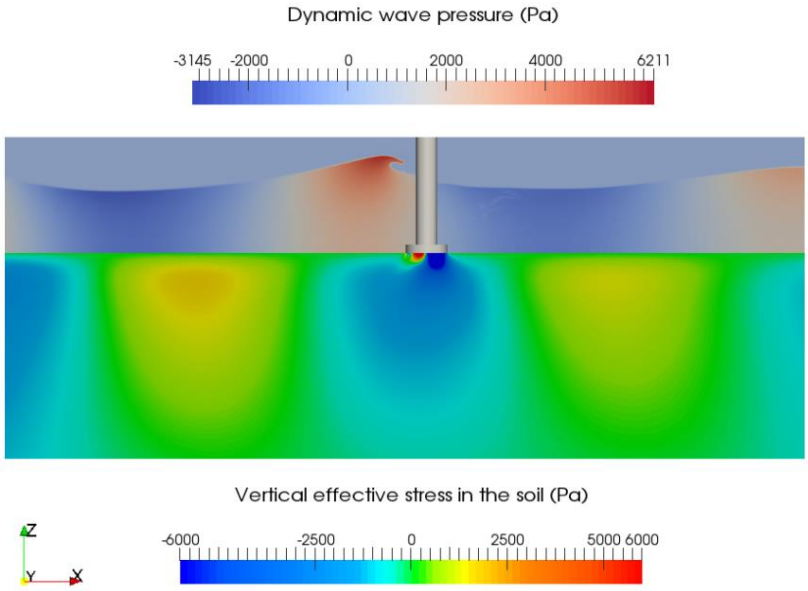

Figure 13: WSI simulation coupled with the response of seabed (the lower part) [152].

The soil models for wave-structure-soil interactions have been built based on the constitutive models developed for onshore geotechnical engineering. Most studies have been performed based on Biot's [150] consolidation model and its extensions. In fact, the seabed is under seawater and subjected to complicated environmental loads such as waves, current and seismic loadings. To date, a generally appropriate seabed constitutive model for marine geotechnical engineering is not yet available in the public literature. Whether the constitutive relations for onshore can be applied to offshore remains to be investigated. Meanwhile, most of the existing works have also been limited to an uncoupled approach or semi-coupled approach, rather than a fully-coupled approach. As the seabed deformed under strong environmental loading or the structure moved its place, it will affect the wave fields and loading distributions in return. Under

circumstances such as complete liquefaction failures and large deformations, the soil can no longer sustain the structure and the structure will move significantly. Therefore, a fully-coupled model with strong two-way interaction of the wave-structure-soil system is necessary to be developed in future.

4. Wave energy converters

In recent years, marine renewable energy systems, such as WECs, supports the global efforts to adopt clean energies. WECs feature unique characteristics, such as aiming at enhanced body motion to extract maximum energy. The large wave conditions and system dynamics of WECs involve significant hydrodynamic non-linear effects, which means linear or weakly non-linear potential flow methods are not suitable. Therefore, OpenFOAM WSI developments are particularly valuable for the modelling of WECs.

4.1 WEC types

In recent years, different devices have been envisaged to exploit and harness the wave energy resource. Figure 14 shows some of the most prominent [159]. Based on different modelling approaches, the following section will divide WECs into four categories, i.e. point absorbers, oscillating wave surge converters (OWSCs), oscillating water columns (OWCs), and flexible WECs. For a specific review of various aspects of WEC modelling in CFD, the interested reader is referred to [21].

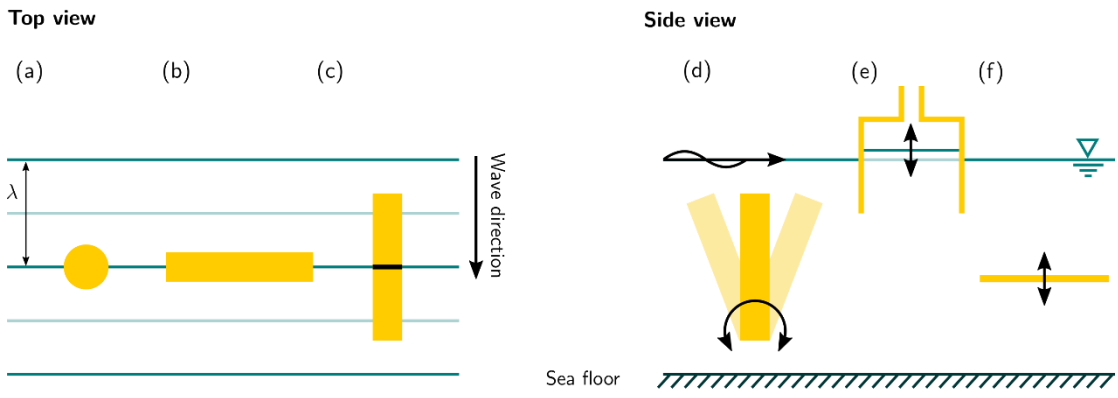

Figure 14: Schematic of different WEC types: (a) Point absorber; (b) Terminator; (c) Attenuator; (d) OWSC; (e) OWC; (f) Pressure differential [21].

4.1.1 Point absorbers

Point absorbers (PAs, Figure 14(a)) are characterised by their small size relative to the incident wavelength. The large device motion due to the action of energy maximising control systems [160] challenges the dynamic mesh motion methods [161]. Numerous studies can be found analysing PAs in the OpenFOAM framework. Studies are conducted in order to, e.g., validate numerical models [162,19,20], evaluate viscous drag effects [163,164], analyse the device performance [165], investigate device scaling [166], assess WEC control performance [59], or for conceptual device design [167].

4.1.2 Oscillating water columns

Within OWCs (Figure 14(e)), the oscillating water level inside a chamber forces entrapped air to rotate a turbine. When modelling these devices in a CFD framework both highly non-linear free surface deformations within the air chamber (i.e. sloshing) [168] and air compressibility [27] may need to be considered. Furthermore, the implementation of the PTO system is of relevance, which can be achieved, e.g., by modelling a narrow orifice [53,169,170] or implementing a porous material in a specific zone of the domain [171] to model the pressure drop over the turbine of the real system. CFD models can then be used for performance assessment [172] or geometry optimisation studies [173,174].

4.1.3 Oscillating wave surge converters

OWSCs (Figure 14(d)) rotate around a hinge point, extracting power from the surging wave motion. While point absorbers are often characterised by multiple operational DoFs, OWSCs feature large excursions in a single Degree of Freedom, pitch. For the modelling of these devices in the OpenFOAM framework, special treatment of the body motion is required, e.g. by using arbitrary mesh interfaces [92,175,176] An example of the use of mesh morphing during the analysis of an OWSC can be found in [177]. Figure 15 shows Benites-Munoz et al.'s work modelling the large rotation of an OWSC using the *overInterDymFoam* [99].

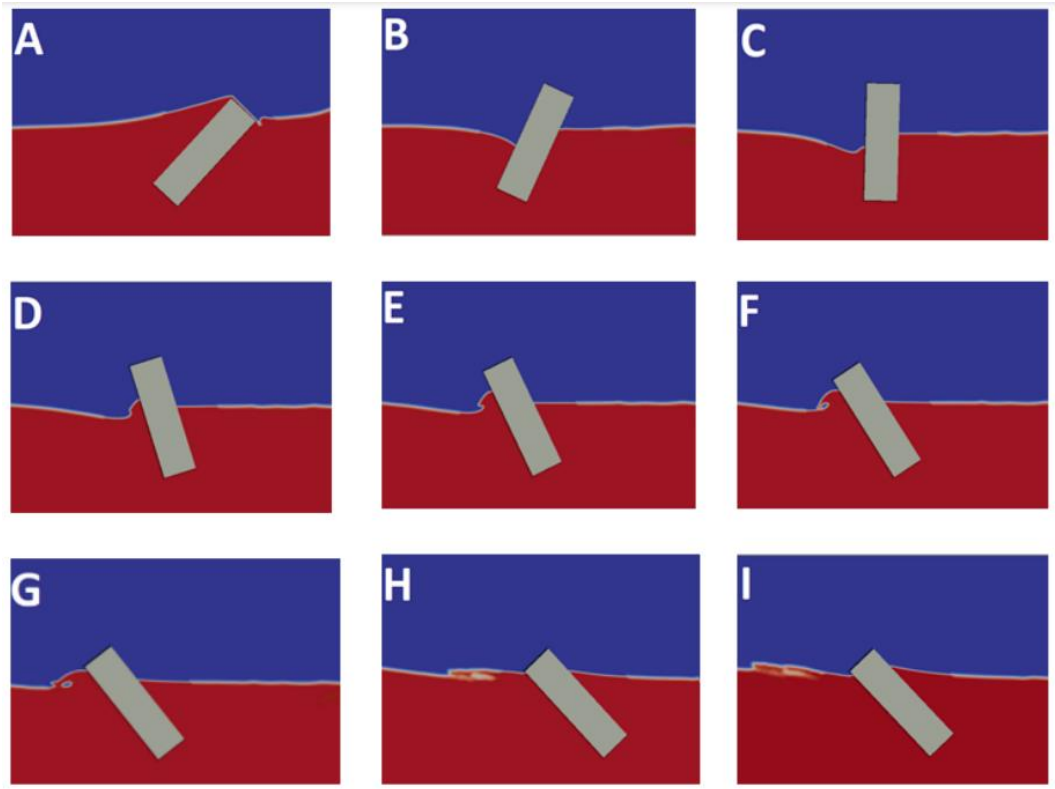

Figure 15: Wave interaction with an oscillating wave energy converter [99]

4.1.4 Flexible WECs

The above rigid types of WECs have suffered from structural problems induced by large wave loads and insufficient energy output [178]. One potential solution can be applying flexible materials for WECs, since the flexibility can effectively mitigate wave loads and the wave-induced deformation can be utilised to generate significant power [178]. Some examples of flexible WEC devices are shown in Figure 16. The functionality of flexible WECs involves complex structural deformations that are based on fully-coupled FSI, i.e., any deformation of the structure triggers a response of the wave flow and vice versa; in the WEC field, a modelling method with such capability has not been seen in literature, which is pointed out as a crucial gap by the recent review of Collins et al. [179]. Fully-coupled FSI can be achieved through CFD+CSM, as introduced in Section 3.3. *Solids4foam* may be a good platform to develop models for flexible WECs; this is demonstrated through a recent work of Huang et al. using fully-coupled CFD+CSM to simulate a "strip shape" WEC [180]. Figure 17 shows the solver's capability of coupling the wave flow and the WEC deformation.

Anaconda, UK SBM S3, France

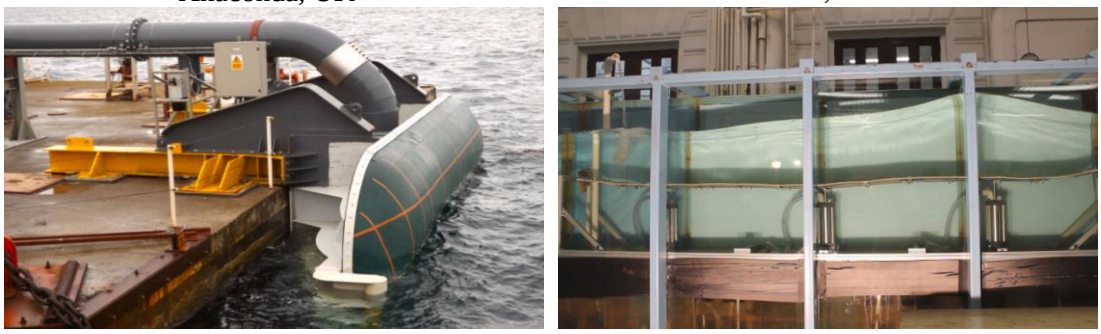

AWS-III, UK Wave Carpet, USA

Figure 16: Flexible WECs: commercial examples

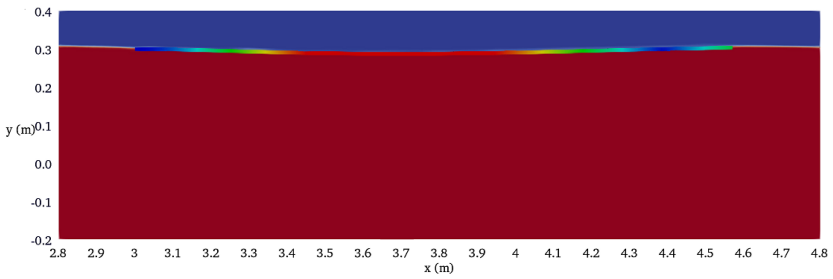

(b) Simulation: floating case

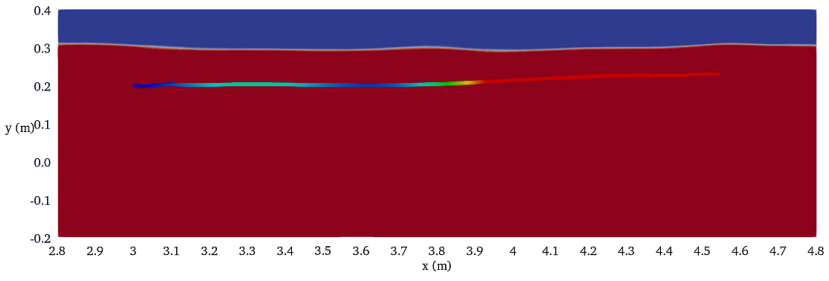

(c) Simulation: submerged case

Figure 17: Wave interaction with a deformable wave energy converter [180].

4.2 Sub-system modelling

In addition to the (floating) structure of a WEC, other sub-system components are relevant,

when analysing WECs and, thus, should ideally be included in the hydrodynamic modelling framework. The most prominent sub-systems are the PTO system (often in conjunction with the energy maximising control system) and the mooring system. When including these sub-systems within the CFD-based NWT, high-fidelity models are desirable, to avoid spoiling the underlying fidelity of the (costly) hydrodynamic model.

4.2.1 Power take-off and control modelling

Including a PTO system within the NWT is inherently required in order to assess the power output of a device. Hence, PTO systems have historically been the first sub-systems to be included within NWTs. As stated in Section 4.1.3, when modelling OWCs, the PTO can simply be mimicked by incorporating a narrow orifice or porous media. For PAs (or OWSCs) a simple implementation of a PTO can be realised by means of a linear spring-damper system, examples of which can be found in, e.g. [105,175,181]. Non-linear PTO representation (with or without the inclusion of energy maximising control systems) is more challenging in terms of their implementation. Coulomb type dampers are implemented in [17,76]. Penalba et al. [182] present the coupling between an OpenFOAM-based NWT with a fully-nonlinear PTO model, running in MATLAB.

4.2.2 Mooring modelling

More recently, the inclusion of mooring systems within NWTs is attracting increased attention. As for the PTO models, different mooring models, with different levels of fidelity and different levels of associated computational cost, are available. A relatively simple implementation of a mooring system can be realised through linear springs, i.e. by simply adding a force that is proportional to the structure displacement [19,20]. For more sophisticated, non-linear mooring models, coupling of the NWT to external toolboxes is commonly used, examples of which can be found in [94,183]. Available mooring toolboxes for OpenFOAM include *MooDy* [184] and *MoorDyn* [185]. Chen and Hall [186] compared these two toolboxes and found their accuracies are very similar. However, *MooDy* applies a finite-element approach that is slower than *MoorDyn*, which applies a lumped mass approach. Apart from considering the structural response in waves, *MooDy* also provides the capability to assess the snap loads in mooring cables, important for the robustness of mooring systems themselves [187].

5. Conclusions

The present paper has reviewed the progress of various WSI modelling approaches in OpenFOAM. The numerical modelling of ocean surface waves and their interactions with fixed, floating, deformable or porous structures have been described in detail. Various available modelling approaches are suggested, and their pros/cons are discussed.

This paper is the first review of WSI modelling for OpenFOAM that has covered such comprehensive topics. To the best knowledge of the authors, this is also potentially the latest and widest WSI review in the entire CFD community. This contribution is expected to help readers better understand the relevant CFD methodologies and provide directions on the selection of models as well as the future development of the field.

References

[1] A.E. Heins, Water waves over a channel of finite depth with a submerged plane barrier, Canadian Journal of Mathematics. 2 (1950) 210–222.

[2] J.R. Morison, J.W. Johnson, S.A. Schaaf, The force exerted by surface waves on piles, Journal of Petroleum Technology. 2 (1950) 149–154.

[3] J.B. Keller, F.C. Karal Jr, Surface wave excitation and propagation, Journal of Applied Physics. 31 (1960) 1039–1046.

[4] R.C.T. Rainey, A new equation for calculating wave loads on offshore structures, Journal of Fluid Mechanics. 204 (1989) 295–324.

[5] O.M. Faltinsen, J.N. Newman, T. Vinje, Nonlinear wave loads on a slender vertical cylinder, Journal of Fluid Mechanics. 289 (1995) 179–198.

[6] B.Z. Zhou, G.X. Wu, Resonance of a tension leg platform exited by third-harmonic force in nonlinear regular waves, Philosophical Transactions of the Royal Society A: Mathematical, Physical and Engineering Sciences. 373 (2015) 20140105.

[7] B.Z. Zhou, G.X. Wu, B. Teng, Fully nonlinear wave interaction with freely floating non-wall-sided structures, Engineering Analysis with Boundary Elements. 50 (2015) 117–132.

[8] Y. Sun, G. Xi, Z. Sun, A fully Lagrangian method for fluid–structure interaction problems with deformable floating structure, Journal of Fluids and Structures. 90 (2019) 379–395.

[9] M.S. Shadloo, G. Oger, D. Le Touzé, Smoothed particle hydrodynamics method for fluid flows, towards industrial applications: Motivations, current state, and challenges, Computers & Fluids. 136 (2016) 11–34.

[10] P. Higuera, olaFlow: CFD for waves [Software]., (2017). https://doi.org/10.5281/zenodo.1297013.

[11] H. Bihs, W. Wang, C. Pakozdi, A. Kamath, REEF3D:: FNPF—A flexible fully nonlinear potential flow solver, Journal of Offshore Mechanics and Arctic Engineering. 142 (2020).

[12] T.R. Keen, T.J. Campbell, J.D. Dykes, P.J. Martin, Gerris Flow Solver: Implementation and Application, NAVAL RESEARCH LAB STENNIS DETACHMENT STENNIS SPACE CENTER MS OCEANOGRAPHY DIV, 2013.

[13] D.M. Greaves, Viscous waves and wave-structure interaction in a tank using adapting quadtree grids, Journal of Fluids and Structures. 23 (2007) 1149–1167.

[14] J. Sanders, J.E. Dolbow, P.J. Mucha, T.A. Laursen, A new method for simulating rigid body motion in incompressible two-phase flow, International Journal for Numerical Methods in Fluids. 67 (2011) 713–732.

[15] J. Westphalen, D.M. Greaves, A. Raby, Z.Z. Hu, D.M. Causon, C.G. Mingham, P. Omidvar, P.K. Stansby, B.D. Rogers, Investigation of wave-structure interaction using

state of the art CFD techniques, Open Journal of Fluid Dynamics. 4 (2014) 18.
[16] L. Sjökvist, M. Göteman, Peak forces on wave energy linear generators in tsunami and extreme waves, Energies. 10 (2017) 1323.
[17] L. Sjökvist, J. Wu, E. Ransley, J. Engström, M. Eriksson, M. Göteman, Numerical models for the motion and forces of point-absorbing wave energy converters in extreme waves, Ocean Engineering. 145 (2017) 1–14. https://doi.org/10.1016/j.oceaneng.2017.08.061.
[18] E. Ransley, S. Yan, S.A. Brown, T. Mai, D. Graham, Q. Ma, P.-H. Musiedlak, A.P. Engsig-Karup, C. Eskilsson, Q. Li, A blind comparative study of focused wave interactions with a fixed FPSO-like structure (CCP-WSI Blind Test Series 1), International Journal of Offshore and Polar Engineering. 29 (2019) 113–127.
[19] E. Ransley, S. Yan, S. Brown, M. Hann, D. Graham, C. Windt, P. Schmitt, J. Davidson, J. Ringwood, P.-H. Musiedlak, A blind comparative study of focused wave interactions with floating structures (CCP-WSI Blind Test Series 3), International Journal of Offshore and Polar Engineering. 30 (2020) 1–10.
[20] E.J. Ransley, S.A. Brown, M. Hann, D.M. Greaves, C. Windt, J. Ringwood, J. Davidson, P. Schmitt, S. Yan, J.X. Wang, J.H. Wang, Q. Ma, Z. Xie, G. Giorgi, J. Hughes, A. Williams, I. Masters, Z. Lin, H. Chen, L. Qian, Z. Ma, Q. Chen, H. Ding, J. Zang, J. van Rij, Y.-H. Yu, Z. Li, B. Bouscasse, G. Ducrozet, H. Bingham, Focused wave interactions with floating structures: a blind comparative study, Proceedings of the Institution of Civil Engineers - Engineering and Computational Mechanics. 174 (2021) 46–61. https://doi.org/10.1680/jencm.20.00006.
[21] C. Windt, J. Davidson, J.V. Ringwood, High-fidelity numerical modelling of ocean wave energy systems: A review of computational fluid dynamics-based numerical wave tanks, Renewable and Sustainable Energy Reviews. 93 (2018) 610–630. https://doi.org/10.1016/j.rser.2018.05.020.
[22] P. Schmitt, C. Windt, J. Davidson, J.V. Ringwood, T. Whittaker, Beyond VoF: alternative OpenFOAM solvers for numerical wave tanks, Journal of Ocean Engineering and Marine Energy. 6 (2020) 277–292.
[23] H. Yang, J. Lu, S. Yan, Preliminary numerical study on oil spilling from a DHT, in: The Twenty-Fourth International Ocean and Polar Engineering Conference, OnePetro, 2014.
[24] F. Gao, Z.H. Ma, J. Zang, D.M. Causon, C.G. Mingham, L. Qian, Simulation of breaking wave impact on a vertical wall with a compressible two-phase flow, model, in: The Twenty-Fifth International Ocean and Polar Engineering Conference, OnePetro, 2015.
[25] B.R. Seiffert, R.C. Ertekin, I.N. Robertson, Wave loads on a coastal bridge deck and the role of entrapped air, Applied Ocean Research. 53 (2015) 91–106.
[26] P.M. Ferrer, D.M. Causon, L. Qian, C.G. Mingham, Z.H. Ma, Numerical simulation of wave slamming on a flap type oscillating wave energy device, Proceedings of the Twentysixth. (2016).
[27] I. Simonetti, L. Cappietti, H. Elsafti, H. Oumeraci, Evaluation of air compressibility effects on the performance of fixed OWC wave energy converters using CFD modelling, Renewable Energy. 119 (2018) 741–753.
[28] I. López, R. Carballo, F. Taveira-Pinto, G. Iglesias, Sensitivity of OWC performance to air compressibility, Renewable Energy. 145 (2020) 1334–1347.
[29] C. Eskilsson, J. Palm, J.P. Kofoed, E. Friis-Madsen, CFD study of the overtopping discharge of the Wave Dragon wave energy converter, Renewable Energies Offshore. (2015) 287–294.
[30] J. Roenby, H. Bredmose, H. Jasak, A computational method for sharp interface advection, Royal Society Open Science. 3 (2016) 160405.
[31] S.S. Deshpande, L. Anumolu, M.F. Trujillo, Evaluating the performance of the two-phase flow solver interFoam, Computational Science & Discovery. 5 (2012) 014016.
[32] B.E. Larsen, D.R. Fuhrman, J. Roenby, Performance of interFoam on the simulation of progressive waves, Coastal Engineering Journal. 61 (2019) 380–400.
[33] V. Vukčević, J. Roenby, I. Gatin, H. Jasak, A sharp free surface finite volume method applied to gravity wave flows, ArXiv Preprint ArXiv:1804.01130. (2018).

[34] V. Vukčević, H. Jasak, I. Gatin, Implementation of the ghost fluid method for free surface flows in polyhedral finite volume framework, Computers & Fluids. 153 (2017) 1–19.
[35] P. Peltonen, P. Kanninen, E. Laurila, V. Vuorinen, The ghost fluid method for openfoam: A comparative study in marine context, Ocean Engineering. 216 (2020) 108007.
[36] CFD Direct, Interface Capturing in OpenFOAM, (2020). https://cfd.direct/openfoam/free-software/multiphase-interface-capturing/.
[37] J.S. Piña, D. Godino, S. Corzo, D. Ramajo, AIR INJECTION IN VERTICAL WATER COLUMN: EXPERIMENTAL TEST AND NUMERICAL SIMULATION USING VOLUME OF FLUID AND TWO-FLUID METHODS, Chemical Engineering Science. (2022) 117665.
[38] A.J.-C. de Saint-Venant, Théorie du mouvement non-permanent des eaux, avec application aux crues des rivieres eta l'introduction des marées dans leur lit, CR Acad. Sci. Paris. 73 (1871) 5.
[39] Ž. Tuković, H. Jasak, A moving mesh finite volume interface tracking method for surface tension dominated interfacial fluid flow, Computers & Fluids. 55 (2012) 70–84.
[40] L. Huang, G. Thomas, Simulation of Wave Interaction With a Circular Ice Floe, Journal of Offshore Mechanics and Arctic Engineering. 141 (2019) 041302.
[41] L.F. Chen, J. Zang, A.J. Hillis, G.C.J. Morgan, A.R. Plummer, Numerical investigation of wave–structure interaction using OpenFOAM, Ocean Engineering. 88 (2014) 91–109.
[42] ITTC, Seakeeping Experiments, Recommended Procedures and Guidelines. (2017).
[43] Y. Li, B. Larsen, D.R. Fuhrman, Reynolds stress turbulence modelling of surf zone breaking waves, Journal of Fluid Mechanics. (2020).
[44] Y.P. Li, D.R. Fuhrman, CFD Simulation of Deep-Water Wave Instabilities Involving Wave Breaking, Journal of Offshore Mechanics and Arctic Engineering. (2021) 1–14.
[45] S. Lyu, L. Huang, G. Thomas, Motions of a Floating Body Induced by Rogue Waves, The 14th OpenFOAM Workshop. (2019).
[46] H. Bredmose, N.G. Jacobsen, Breaking wave impacts on offshore wind turbine foundations: focused wave groups and CFD, in: International Conference on Offshore Mechanics and Arctic Engineering, 2010: pp. 397–404.
[47] P. Schmitt, B. Elsaesser, On the use of OpenFOAM to model oscillating wave surge converters, Ocean Engineering. 108 (2015) 98–104. https://doi.org/10.1016/j.oceaneng.2015.07.055.
[48] P. Higuera, I.J. Losada, J.L. Lara, Three-dimensional numerical wave generation with moving boundaries, Coastal Engineering. 101 (2015) 35–47.
[49] P. Schmitt, B. Elsaesser, A Review of Wave Makers for 3D Numerical Simulations, VI International Conference on Computational Methods in Marine Engineering (MARINE 2015). (2015) 1–10.
[50] C. Windt, J. Davidson, P. Schmitt, J. V Ringwood, Assessment of Numerical Wave Makers, (2017).
[51] N.G. Jacobsen, D.R. Fuhrman, J. Fredsøe, A wave generation toolbox for the open-source CFD library: OpenFoam®, International Journal for Numerical Methods in Fluids. 70 (2012) 1073–1088. https://doi.org/10.1002/fld.2726.
[52] Z.Z. Hu, D. Greaves, A. Raby, Numerical wave tank study of extreme waves and wave-structure interaction using OpenFoam®, Ocean Engineering. 126 (2016) 329–342.
[53] T. Vyzikas, S. Deshoulières, O. Giroux, M. Barton, D. Greaves, Numerical study of fixed Oscillating Water Column with RANS-type two-phase CFD model, Renewable Energy. 102 (2017) 294–305.
[54] N. Bruinsma, B.T. Paulsen, N.G. Jacobsen, Validation and application of a fully nonlinear numerical wave tank for simulating floating offshore wind turbines, Ocean Engineering. 147 (2018) 647–658.
[55] N. Bruinsma, Validation and application of a fully nonlinear numerical wave tank, (2016).
[56] IHCantabria, IHFoam manual, 2014. https://ihfoam.ihcantabria.com/.
[57] B. Devolder, P. Rauwoens, P. Troch, Application of a buoyancy-modified k-$ømega$ SST turbulence model to simulate wave run-up around a monopile subjected to

regular waves using OpenFOAM®, Coastal Engineering. 125 (2017) 81–94.
[58] H.G. Guler, C. Baykal, T. Arikawa, A.C. Yalciner, Numerical assessment of tsunami attack on a rubble mound breakwater using OpenFOAM®, Applied Ocean Research. 72 (2018) 76–91.
[59] C. Windt, N. Faedo, M. Penalba, F. Dias, J.V. Ringwood, Reactive control of wave energy devices–the modelling paradox, Applied Ocean Research. 109 (2021) 102574.
[60] P. Higuera, J.L. Lara, I.J. Losada, Realistic wave generation and active wave absorption for Navier-Stokes models. Application to OpenFOAM®., Coastal Engineering. 71 (2013) 102–118. https://doi.org/10.1016/j.coastaleng.2012.07.002.
[61] IHCantabria, IHFOAM Manual 15th July 2014, (2014).
[62] H.A. Schäffer, G. Klopman, Review of multidirectional active wave absorption methods, Journal of Waterway, Port, Coastal, and Ocean Engineering. 126 (2000) 88–97.
[63] P. Higuera, Enhancing active wave absorption in RANS models, Applied Ocean Research. 94 (2020) 102000.
[64] M. Borsboom, N.G. Jacobsen, A generating-absorbing boundary condition for dispersive waves, International Journal for Numerical Methods in Fluids. 93 (2021) 2443–2467.
[65] C. Windt, J. Davidson, P. Schmitt, J. V. Ringwood, On the Assessment of Numerical Wave Makers in CFD simulations, Journal of Marine Science and Engineering. 7 (2019). https://doi.org/10.3390/JMSE7020047.
[66] K.O. Connell, A. Cashman, Development of a numerical wave tank with reduced discretization error, in: 2016 International Conference on Electrical, Electronics, and Optimization Techniques (ICEEOT), IEEE, 2016: pp. 3008–3012.
[67] P. Schmitt, B. Elsaesser, A review of wave makers for 3D numerical simulations, in: MARINE VI: Proceedings of the VI International Conference on Computational Methods in Marine Engineering, CIMNE, 2015: pp. 437–446.
[68] C. Windt, J. Davidson, P. Schmitt, J.V. Ringwood, On the assessment of numerical wave makers in CFD simulations, Journal of Marine Science and Engineering. 7 (2019) 47.
[69] B. Pena, L. Huang, A review on the turbulence modelling strategy for ship hydrodynamic simulations, Ocean Engineering. (2021).
[70] J. Davidson, R. Costello, Efficient nonlinear hydrodynamic models for wave energy converter design—A scoping study, Journal of Marine Science and Engineering. 8 (2020) 35.
[71] D. Khojasteh, S. Tavakoli, A. Dashtimanesh, A. Dolatshah, L. Huang, W. Glamore, M. Sadat-Noori, G. Iglesias, Numerical analysis of shipping water impacting a step structure, Ocean Engineering. 209 (2020) 107517.
[72] C. Windt, J. Davidson, J.V. Ringwood, Investigation of Turbulence Modeling for Point-Absorber-Type Wave Energy Converters, Energies. 14 (2021) 26.
[73] Y. Li, M.B. Fredberg, B.E. Larsen, D.R. Fuhrman, Simulating Breaking Waves with the Reynolds Stress Turbulence Model, Coastal Engineering Proceedings. (2020) 17–17.
[74] D.R. Fuhrman, Y. Li, Instability of the realizable k–ε turbulence model beneath surface waves, Physics of Fluids. 32 (2020) 115108.
[75] S.A. Brown, D.M. Greaves, V. Magar, D.C. Conley, Evaluation of turbulence closure models under spilling and plunging breakers in the surf zone, Coastal Engineering. 114 (2016) 177–193.
[76] B. Devolder, V. Stratigaki, P. Troch, P. Rauwoens, CFD Simulations of Floating Point Absorber Wave Energy Converter Arrays Subjected to Regular Waves, Energies. 11 (2018) 641. https://doi.org/10.3390/en11030641.
[77] B.E. Larsen, D.R. Fuhrman, On the over-production of turbulence beneath surface waves in Reynolds-averaged Navier–Stokes models, Journal of Fluid Mechanics. 853 (2018) 419–460.
[78] Y. Li, The Reynolds Stress Turbulence Model, https://github.com/LiYZPearl/ReynoldsStressTurbulenceModels., 2021.
[79] Y. Li, M.C. Ong, T. Tang, Numerical analysis of wave-induced poro-elastic seabed response around a hexagonal gravity-based offshore foundation, Coastal Engineering.

136 (2018) 81–95.
[80] M. Mortazavi, V. Le Chenadec, P. Moin, A. Mani, Direct numerical simulation of a turbulent hydraulic jump: turbulence statistics and air entrainment, Journal of Fluid Mechanics. 797 (2016) 60–94.
[81] P. Lopes, J. Leandro, R.F. Carvalho, Self-aeration modelling using a sub-grid volume-of-fluid model, International Journal of Nonlinear Sciences and Numerical Simulation. 18 (2017) 559–574.
[82] J. Ma, A.A. Oberai, D.A. Drew, R.T. Lahey Jr, M.C. Hyman, A comprehensive sub-grid air entrainment model for RaNS modeling of free-surface bubbly flows, The Journal of Computational Multiphase Flows. 3 (2011) 41–56.
[83] P.D. Tomaselli, A methodology for air entrainment in breaking waves and their interaction with a mono-pile, PhD Thesis, Technical University of Denmark Lyngby, Denmark, 2016.
[84] G. Morgan, J. Zang, Application of OpenFOAM to coastal and offshore modelling, The 26th IWWWFB. Athens, Greece. (2011).
[85] W. Chen, J.J. Warmink, M.R.A. Van Gent, S. Hulscher, Numerical modelling of wave overtopping at dikes using OpenFOAM®, Coastal Engineering. 166 (2021) 103890.
[86] B. Di Paolo, J.L. Lara, G. Barajas, Í.J. Losada, Wave and structure interaction using multi-domain couplings for Navier-Stokes solvers in OpenFOAM®. Part I: Implementation and validation, Coastal Engineering. 164 (2021) 103799. https://doi.org/10.1016/j.coastaleng.2020.103799.
[87] B. Di Paolo, J.L. Lara, G. Barajas, Í.J. Losada, Waves and structure interaction using multi-domain couplings for Navier-Stokes solvers in OpenFOAM®. Part II: Validation and application to complex cases, Coastal Engineering. 164 (2021) 103818. https://doi.org/10.1016/j.coastaleng.2020.103818.
[88] G. Ducrozet, F. Bonnefoy, D. Le Touzé, P. Ferrant, A modified high-order spectral method for wavemaker modeling in a numerical wave tank, European Journal of Mechanics-B/Fluids. 34 (2012) 19–34.
[89] B. Quinn, Validation of the High Order Spectral (HOS) Method for Extreme and Breaking Waves and Coupling of the HOS-Numerical Wave Tank Model with OpenFOAM, Master's Thesis, University of Stavanger, Norway, 2019.
[90] G. Decorte, A. Toffoli, G. Lombaert, J. Monbaliu, On the use of a domain decomposition strategy in obtaining response statistics in non-Gaussian seas, Fluids. 6 (2021) 28.
[91] S. Tavakoli, A.V. Babanin, Wave energy attenuation by drifting and non-drifting floating rigid plates, Ocean Engineering. 226 (2021) 108717. https://doi.org/10.1016/j.oceaneng.2021.108717.
[92] P. Schmitt, B. Elsaesser, On the use of OpenFOAM to model oscillating wave surge converters, Ocean Engineering. 108 (2015) 98–104. https://doi.org/10.1016/j.oceaneng.2015.07.055.
[93] J. Palm, C. Eskilsson, Facilitating Large-Amplitude Motions of Wave Energy Converters in OpenFOAM by a Modified Mesh Morphing Approach, in: 14th European Wave and Tidal Energy Conference, European Tidal and Wave Energy Conference, 2021.
[94] J. Palm, C. Eskilsson, G.M. Paredes, L. Bergdahl, Coupled mooring analysis for floating wave energy converters using CFD: Formulation and validation, International Journal of Marine Energy. 16 (2016) 83–99.
[95] H. Islam, S.C. Mohapatra, J. Gadelho, C.G. Soares, OpenFOAM analysis of the wave radiation by a box-type floating structure, Ocean Engineering. 193 (2019) 106532.
[96] M. Yan, X. Ma, W. Bai, Z. Lin, Y. Li, Numerical simulation of wave interaction with payloads of different postures using OpenFOAM, Journal of Marine Science and Engineering. 8 (2020) 433.
[97] S.C. Mohapatra, H. Islam, C. Guedes Soares, Boussinesq model and CFD simulations of non-linear wave diffraction by a floating vertical cylinder, Journal of Marine Science and Engineering. 8 (2020) 575.
[98] M. Yousefifard, A. Graylee, A numerical solution of the wave–body interactions for a

freely floating vertical cylinder in different water depths using OpenFOAM, Journal of the Brazilian Society of Mechanical Sciences and Engineering. 43 (2021) 1–14.
[99] D. Benites-Munoz, L. Huang, E. Anderlini, J.R. Marín-Lopez, G. Thomas, Hydrodynamic Modelling of An Oscillating Wave Surge Converter Including Power Take-Off, Journal of Marine Science and Engineering. 8 (2020) 771.
[100] L. Huang, S. Tavakoli, M. Li, A. Dolatshah, B. Pena, B. Ding, A. Dashtimanesh, CFD analyses on the water entry process of a freefall lifeboat, Ocean Engineering. 232 (2021) 109115.
[101] H. Chen, L. Qian, Z. Ma, W. Bai, Y. Li, D. Causon, C. Mingham, Application of an overset mesh based numerical wave tank for modelling realistic free-surface hydrodynamic problems, Ocean Engineering. 176 (2019) 97–117.
[102] D.D. Chandar, On overset interpolation strategies and conservation on unstructured grids in openfoam, Computer Physics Communications. 239 (2019) 72–83.
[103] T. Wu, W. Luo, D. Jiang, R. Deng, S. Huang, Numerical Study on Wave-Ice Interaction in the Marginal Ice Zone, Journal of Marine Science and Engineering. 9 (2021) 4.
[104] C. Windt, J. Davidson, B. Akram, J.V. Ringwood, Performance assessment of the overset grid method for numerical wave tank experiments in the OpenFOAM environment, in: International Conference on Offshore Mechanics and Arctic Engineering, American Society of Mechanical Engineers, 2018: p. V010T09A006.
[105] C. Windt, J. Davidson, E.J. Ransley, D. Greaves, M. Jakobsen, M. Kramer, J.V. Ringwood, Validation of a CFD-based numerical wave tank model for the power production assessment of the wavestar ocean wave energy converter, Renewable Energy. 146 (2020) 2499–2516.
[106] J.R. Chaplin, V. Heller, F.J.M. Farley, G.E. Hearn, R.C.T. Rainey, Laboratory testing the Anaconda, Philosophical Transactions of the Royal Society A: Mathematical, Physical and Engineering Sciences. 370 (2012) 403–424.
[107] L. Huang, Y. Li, Design of the submerged horizontal plate breakwater using a fully coupled hydroelastic approach, Computer-Aided Civil and Infrastructure Engineering. (2021).
[108] L. Huang, K. Ren, M. Li, Ž. Tuković, P. Cardiff, G. Thomas, Fluid-structure interaction of a large ice sheet in waves, Ocean Engineering. 182 (2019) 102–111.
[109] N.G. Jacobsen, W. Bakker, W.S. Uijttewaal, R. Uittenbogaard, Experimental investigation of the wave-induced motion of and force distribution along a flexible stem, Journal of Fluid Mechanics. 880 (2019) 1036–1069.
[110] M. Masoomi, A. Mosavi, The One-Way FSI Method Based on RANS-FEM for the Open Water Test of a Marine Propeller at the Different Loading Conditions, Journal of Marine Science and Engineering. 9 (2021) 351.
[111] H. Chen, Q. Zou, Z. Liu, A coupled RANS-VOF and finite element model for wave interaction with highly flexible vegetation, COASTAL ENGINEERING. (2016) 2.
[112] A. Karac, Drop impact of fluid-filled polyethylene containers, PhD Thesis, Imperial College London (University of London), 2003.
[113] C.-G. Giannopapa, Fluid structure interaction in flexible vessels, PhD Thesis, University of London, 2004.
[114] C.J. Greenshields, H.G. Weller, A unified formulation for continuum mechanics applied to fluid–structure interaction in flexible tubes, International Journal for Numerical Methods in Engineering. 64 (2005) 1575–1593.
[115] Z. Tukovic, H. Jasak, Updated Lagrangian finite volume solver for large deformation dynamic response of elastic body, Transactions of FAMENA. 31 (2007) 55.
[116] Z. Tukovic, P. Cardiff, A. Karac, H. Jasak, A. Ivankovic, OpenFOAM library for fluid structure interaction, in: 9th OpenFOAM Workshop, 2014.
[117] Ž. Tuković, A. Ivanković, A. Karač, Finite-volume stress analysis in multi-material linear elastic body, International Journal for Numerical Methods in Engineering. 93 (2013) 400–419.
[118] J. McVicar, J. Lavroff, M.R. Davis, G. Thomas, Fluid–structure interaction simulation of

slam-induced bending in large high-speed wave-piercing catamarans, Journal of Fluids and Structures. 82 (2018) 35–58.
[119] L. Huang, An opensource solver for wave-induced FSI problems, In Proceedings of CFD with OpenSource Software. Edited by Nilsson. H. (2018). http://dx.doi.org/10.17196/OS_CFD#YEAR_2017.
[120] P. Cardiff, A. Karač, P. De Jaeger, H. Jasak, J. Nagy, A. Ivanković, Ž. Tuković, An open-source finite volume toolbox for solid mechanics and fluid-solid interaction simulations, ArXiv Preprint ArXiv:1808.10736. (2018).
[121] T. Tang, O. Hededal, P. Cardiff, On finite volume method implementation of poro-elasto-plasticity soil model, International Journal for Numerical and Analytical Methods in Geomechanics. 39 (2015) 1410–1430.
[122] I. Oliveira, J. Gasche, P. Cardiff, Implementation and numerical verification of an incompressible three-parameter Mooney-Rivlin model for large deformation of soft tissues, in: The 15th OpenFOAM Workshop, 2020.
[123] M. Girfoglio, A. Quaini, G. Rozza, Fluid-structure interaction simulations with a LES filtering approach in solids4Foam, ArXiv Preprint ArXiv:2102.08011. (2021).
[124] M. Abusara, N. Hakan, P. Cardiff, D. Randstrom, Fluid-structure interaction on a fixed fan blade, in: The 16th OpenFOAM Workshop, 2021.
[125] Y. Li, Z. Hu, L. Huang, Hydroelastic Simulation of Breaking Wave Impact on a Flexible Coastal Seawall, in: The 41th International Conference on Ocean, Offshore & Arctic Engineering (OMAE), ASME: The American Society of Mechanical Engineers, 2022.
[126] I.J. Losada, J.L. Lara, M. del Jesus, Modeling the interaction of water waves with porous coastal structures, Journal of Waterway, Port, Coastal, and Ocean Engineering. 142 (2016) 03116003.
[127] F. Mentzoni, T. Kristiansen, A Semi-Analytical Method for Calculating the Hydrodynamic Force on Perforated Plates in Oscillating Flow, in: International Conference on Offshore Mechanics and Arctic Engineering, American Society of Mechanical Engineers, 2019: p. V07AT06A015.
[128] A. George, I.H. Cho, Anti-sloshing effects of a vertical porous baffle in a rolling rectangular tank, Ocean Engineering. 214 (2020) 107871.
[129] S.K. Poguluri, I.H. Cho, Liquid sloshing in a rectangular tank with vertical slotted porous screen: based on analytical, numerical, and experimental approach, Ocean Engineering. 189 (2019) 106373.
[130] K. Shim, P. Klebert, A. Fredheim, Numerical investigation of the flow through and around a net cage, in: International Conference on Offshore Mechanics and Arctic Engineering, 2009: pp. 581–587.
[131] H. Chen, E.D. Christensen, Investigations on the porous resistance coefficients for fishing net structures, Journal of Fluids and Structures. 65 (2016) 76–107.
[132] A. Feichtner, E. Mackay, G. Tabor, P.R. Thies, L. Johanning, D. Ning, Using a porous-media approach for CFD modelling of wave interaction with thin perforated structures, Journal of Ocean Engineering and Marine Energy. 7 (2021) 1–23.
[133] S. Hadadpour, M. Paul, H. Oumeraci, Numerical investigation of wave attenuation by rigid vegetation based on a porous media approach, Journal of Coastal Research. 92 (2019) 92–100.
[134] P. Higuera, J.L. Lara, I.J. Losada, Three-dimensional interaction of waves and porous coastal structures using OpenFOAM®. Part I: Formulation and validation, Coastal Engineering. 83 (2014) 243–258.
[135] P. Higuera, J.L. Lara, I.J. Losada, Three-dimensional interaction of waves and porous coastal structures using OpenFOAM®. Part II: Application, Coastal Engineering. 83 (2014) 259–270.
[136] M. Maza, J.L. Lara, I.J. Losada, Tsunami wave interaction with mangrove forests: A 3-D numerical approach, Coastal Engineering. 98 (2015) 33–54.
[137] A. Feichtner, E. Mackay, G. Tabor, P.R. Thies, L. Johanning, Comparison of Macro-Scale Porosity Implementations for CFD Modelling of Wave Interaction with Thin

Porous Structures, Journal of Marine Science and Engineering. 9 (2021) 150.
[138] B. Jensen, N.G. Jacobsen, E.D. Christensen, Investigations on the porous media equations and resistance coefficients for coastal structures, Coastal Engineering. 84 (2014) 56–72.
[139] N.G. Jacobsen, D.R. Fuhrman, J. Fredsøe, A wave generation toolbox for the open-source CFD library: OpenFoam®, International Journal for Numerical Methods in Fluids. 70 (2012) 1073–1088.
[140] A. Feichtner, E. Mackay, G. Tabor, P.R. Thies, L. Johanning, Modelling wave interaction with thin porous structures using OpenFOAM, in: Proceedings of the 13th European Wave and Tidal Energy Conference (EWTEC 2019), Napoli, Italy, 2019: pp. 1–6.
[141] A. Feichtner, G. Tabor, E. Mackay, P. Thies, L. Johanning, On the use of a porous-media approach for the modelling of wave interaction with thin perforated cylinders, in: The 15th OpenFOAM Workshop (OFW15), Online, 2020.
[142] P. Lin, Numerical modeling of breaking waves, Cornell University, 1998.
[143] P.L.-F. Liu, P. Lin, K.-A. Chang, T. Sakakiyama, Numerical modeling of wave interaction with porous structures, Journal of Waterway, Port, Coastal, and Ocean Engineering. 125 (1999) 322–330.
[144] Y.-T. Wu, S.-C. Hsiao, Propagation of solitary waves over a submerged slotted barrier, Journal of Marine Science and Engineering. 8 (2020) 419.
[145] K.-H. Lee, J.-H. Bae, S.-G. Kim, D.-S. Kim, Three-dimensional simulation of wave reflection and pressure acting on circular perforated caisson breakwater by OLAFOAM, Journal of Korean Society of Coastal and Ocean Engineers. 29 (2017) 286–304.
[146] V.K. Srineash, A. Kamath, K. Murali, H. Bihs, Numerical Simulation of Wave Interaction with Submerged Porous Structures and Application for Coastal Resilience, Journal of Coastal Research. 36 (2020) 752–770.
[147] M. Brito, J. Fernandes, J.B. Leal, Porous media approach for RANS simulation of compound open-channel flows with submerged vegetated floodplains, Environmental Fluid Mechanics. 16 (2016) 1247–1266.
[148] Y.-P. Zhao, C.-W. Bi, Y.-X. Liu, G.-H. Dong, F.-K. Gui, Numerical simulation of interaction between waves and net panel using porous media model, Engineering Applications of Computational Fluid Mechanics. 8 (2014) 116–126.
[149] X. Liu, M.H. García, R. Muscari, Numerical investigation of seabed response under waves with free-surface water flow, International Journal of Offshore and Polar Engineering. 17 (2007).
[150] M.A. Biot, General theory of three-dimensional consolidation, Journal of Applied Physics. 12 (1941) 155–164.
[151] T. Tang, B. Johannesson, An integrated FVM simulation of wave-seabed-structure interaction using OpenFoam, in: 9th OpenFOAM Workshop, 23-26 June 2014 in Zagreb, Croatia, 2014.
[152] Y. Li, M.C. Ong, T. Tang, A numerical toolbox for wave-induced seabed response analysis around marine structures in the OpenFOAM® framework, Ocean Engineering. 195 (2020) 106678.
[153] Z. Lin, D. Pokrajac, Y. Guo, D. Jeng, T. Tang, N. Rey, J. Zheng, J. Zhang, Investigation of nonlinear wave-induced seabed response around mono-pile foundation, Coastal Engineering. 121 (2017) 197–211.
[154] D. Celli, Y. Li, M.C. Ong, M. Di Risio, The role of submerged berms on the momentary liquefaction around conventional rubble mound breakwaters, Applied Ocean Research. 85 (2019) 1–11.
[155] D. Celli, Y. Li, M.C. Ong, M. Di Risio, Random wave-induced momentary liquefaction around rubble mound breakwaters with submerged berms, Journal of Marine Science and Engineering. 8 (2020) 338.
[156] Z. Liang, D.-S. Jeng, PORO-FSSI-FOAM model for seafloor liquefaction around a pipeline under combined random wave and current loading, Applied Ocean Research. 107 (2021) 102497.
[157] J. Ye, K. He, L. Zhou, Subsidence prediction of a rubble mound breakwater at Yantai

port: A application of FSSI-CAS 2D, Ocean Engineering. 219 (2021) 108349.
[158] H. Elsafti, H. Oumeraci, A numerical hydro-geotechnical model for marine gravity structures, Computers and Geotechnics. 79 (2016) 105–129.
[159] European Marine Energy Centre (EMEC), WAVE DEVICES, (2020). http://www.emec.org.uk/marine-energy/wave-devices/.
[160] G. Giorgi, J. Ringwood, Consistency of viscous drag identification tests for wave energy applications, in: Proceedings of the 12th European Wave and Tidal Energy Conference 27th Aug-1st Sept 2017, European Wave and Tidal Energy Conference 2017, 2017: pp. 1–8.
[161] C. Windt, J. Davidson, D.D. Chandar, N. Faedo, J.V. Ringwood, Evaluation of the overset grid method for control studies of wave energy converters in OpenFOAM numerical wave tanks, Journal of Ocean Engineering and Marine Energy. 6 (2020) 55–70.
[162] E.J. Ransley, D.M. Greaves, A. Raby, D. Simmonds, M.M. Jakobsen, M. Kramer, RANS-VOF modelling of the Wavestar point absorber, Renewable Energy. 109 (2017) 49–65. https://doi.org/10.1016/j.renene.2017.02.079.
[163] J. Palm, C. Eskilsson, L. Bergdahl, R.E. Bensow, Assessment of Scale Effects, Viscous Forces and Induced Drag on a Point-Absorbing Wave Energy Converter by CFD Simulations, Journal of Marine Science and Engineering. 6 (2018) 124. https://doi.org/10.3390/jmse6040124.
[164] B.W. Schubert, F. Meng, N.Y. Sergiienko, W. Robertson, B.S. Cazzolato, M.H. Ghayesh, A. Rafiee, B. Ding, M. Arjomandi, Pseudo-nonlinear hydrodynamic coefficients for modelling point absorber wave energy converters, in: Proceedings of the 4th Asian Wave and Tidal Energy Conference, Taipei, Taiwan, 2018: pp. 9–13.
[165] F. Meng, A. Rafiee, B. Ding, B. Cazzolato, M. Arjomandi, Nonlinear hydrodynamics analysis of a submerged spherical point absorber with asymmetric mass distribution, Renewable Energy. 147 (2020) 1895–1908. https://doi.org/10.1016/j.renene.2019.09.101.
[166] C. Windt, J. Davidson, J.V. Ringwood, Numerical analysis of the hydrodynamic scaling effects for the Wavestar wave energy converter, Journal of Fluids and Structures. 105 (2021) 103328. https://doi.org/10.1016/j.jfluidstructs.2021.103328.
[167] H. Akimoto, K. Tanaka, Y.Y. Kim, Drag-type cross-flow water turbine for capturing energy from the orbital fluid motion in ocean wave, Renewable Energy. 76 (2015) 196–203. https://doi.org/10.1016/j.renene.2014.11.016.
[168] C. Xu, Z. Huang, Three-dimensional CFD simulation of a circular OWC with a nonlinear power-takeoff: Model validation and a discussion on resonant sloshing inside the pneumatic chamber, Ocean Engineering. 176 (2019) 184–198. https://doi.org/10.1016/j.oceaneng.2019.02.010.
[169] A. Iturrioz, R. Guanche, J.L. Lara, C. Vidal, I.J. Losada, Validation of OpenFOAM® for Oscillating Water Column three-dimensional modeling, Ocean Engineering. 107 (2015) 222–236. https://doi.org/10.1016/j.oceaneng.2015.07.051.
[170] Z. Deng, C. Wang, P. Wang, P. Higuera, R. Wang, Hydrodynamic performance of an offshore-stationary OWC device with a horizontal bottom plate: Experimental and numerical study, Energy. 187 (2019) 115941. https://doi.org/10.1016/j.energy.2019.115941.
[171] A. Dimakopoulos, M. Cooker, E. Medina-Lopez, D. Longo, R. Pinguet, Flow characterisation and numerical modelling of owc wave energy converters, in: 11th European Wave & Tidal Energy Conference (EWTEC). Nantes, France, 2015.
[172] K. Rezanejad, J.F.M. Gadelho, C. Guedes Soares, Hydrodynamic analysis of an oscillating water column wave energy converter in the stepped bottom condition using CFD, Renewable Energy. 135 (2019) 1241–1259. https://doi.org/10.1016/j.renene.2018.09.034.
[173] I. Simonetti, L. Cappietti, H. El Safti, H. Oumeraci, Numerical modelling of fixed oscillating water column wave energy conversion devices: Toward geometry hydraulic optimization, in: International Conference on Offshore Mechanics and Arctic Engineering, American Society of Mechanical Engineers, 2015: p. V009T09A031.

[174] I. Simonetti, L. Cappietti, H. Elsafti, H. Oumeraci, Optimization of the geometry and the turbine induced damping for fixed detached and asymmetric OWC devices: A numerical study, Energy. 139 (2017) 1197–1209. https://doi.org/10.1016/j.energy.2017.08.033.
[175] T.T. Loh, D. Greaves, T. Maeki, M. Vuorinen, D. Simmonds, A. Kyte, Numerical modelling of the WaveRoller device using OpenFOAM, in: Proceedings of the 3rd Asian Wave & Tidal Energy Conference, 2016.
[176] J.A. Bridgwater Court, D.R.S. Cahndel, A.R. Plummer, A.J. Hillis, Modelling of array interactions for a curved OSWEC using OpenFOAM, in: The 12th European Wave and Tidal Energy Conference (EWTEC), Cork, 2017.
[177] C. Lifen, S.U.N. Liang, Z. Jun, A.J. Hillis, A.R. Plummer, Numerical study of roll motion of a 2-D floating structure in viscous flow, Journal of Hydrodynamics, Ser. B. 28 (2016) 544–563.
[178] E. Renzi, S. Michele, S. Zheng, S. Jin, D. Greaves, Niche applications and flexible devices for wave energy conversion: A review, Energies. 14 (2021) 6537.
[179] I. Collins, M. Hossain, W. Dettmer, I. Masters, Flexible membrane structures for wave energy harvesting: A review of the developments, materials and computational modelling approaches, Renewable and Sustainable Energy Reviews. 151 (2021) 111478.
[180] L. Huang, Z. Hu, Y. Li, G. Thomas, Fully-coupled CFD+CSM analysis on an elastic floating/submerged plate for wave energy harvest, in: 9th International Conference on HYDROELASTICITY IN MARINE TECHNOLOGY, Rome, Italy, 2022.
[181] A. Rafiee, J. Fiévez, Numerical prediction of extreme loads on the CETO wave energy converter, in: Proceedings of the 11th European Wave and Tidal Energy Conference, Nantes, France, 2015.
[182] M. Penalba, J. Davidson, C. Windt, J.V. Ringwood, A high-fidelity wave-to-wire simulation platform for wave energy converters: Coupled numerical wave tank and power take-off models, Applied Energy. 226 (2018) 655–669. https://doi.org/10.1016/j.apenergy.2018.06.008.
[183] C. Jiang, O. el Moctar, G. Moura Paredes, T.E. Schellin, Validation of a dynamic mooring model coupled with a RANS solver, Marine Structures. 72 (2020) 102783. https://doi.org/10.1016/j.marstruc.2020.102783.
[184] J. Palm, C. Eskilsson, MOODY User Manual: version 1.0. 0, (2018).
[185] M. Hall, Moordyn v2: New capabilities in mooring system components and load cases, in: International Conference on Offshore Mechanics and Arctic Engineering, American Society of Mechanical Engineers, 2020: p. V009T09A078.
[186] H. Chen, M. Hall, CFD simulation of floating body motion with mooring dynamics: Coupling MoorDyn with OpenFOAM, Applied Ocean Research. 124 (2022) 103210.
[187] J. Palm, C. Eskilsson, L. Bergdahl, An hp-adaptive discontinuous Galerkin method for modelling snap loads in mooring cables, Ocean Engineering. 144 (2017) 266–276.